Ca^{2+} Fluxes and Channel Regulation in Rods of the Albino Rat

ANDREAS KNOPP and H. RÜPPEL

From the Max Volmer Institut für Biophysikalische and Physikalische Chemie, Technische Universität Berlin, D-10623 Berlin, Germany

ABSTRACT By use of microelectrodes, changes in the receptor current and the Ca^{2+} concentration were measured in the rod layer of the rat retina after stimulation by flashes or steady light. Thereby light induced Ca^{2+} sources, and sinks along a rod were determined in dependence of time. Thus, the Ca^{2+} fluxes across the plasma membrane of a mammalian rod could be studied in detail. By light stimulation, Ca^{2+} sources are evoked along the outer segment only. Immediately after a saturating flash, a maximum of Ca^{2+} efflux is observed which decays exponentially with $\tau = 0.3$ s at 37°C (4.2 s at 23°C). During regeneration of the dark current, the outer segment acts as a Ca^{2+} sink, indicating a restoration of the Ca^{2+}-depleted outer segment. These findings agree with earlier reports on amphibian rods. Further experiments showed that the peak Ca^{2+} efflux and τ are temperature dependent. The peak amplitude also depends on the external Ca^{2+} concentration. In contrast to the reports on amphibian rods, only a part of the Ca^{2+} ions extruded from the outer segment is directly restored. Surprisingly, during steady light the Ca^{2+} efflux approaches a permanent residual value. Therefore, in course of a photoresponse, Ca^{2+} must be liberated irreversibly from internal Ca^{2+} stores. There is certain evidence that the inner segment acts as a Ca^{2+} store. Our results show that the Ca^{2+} fraction of the ions carrying the dark current is proportional to the extracellular Ca^{2+} concentration. This indicates that the Ca^{2+} permeability of the plasma membrane of the rod outer segment is independent of the Ca^{2+} concentration. Key words: rat rod photoreceptors • Ca^{2+}-sensitive microelectrodes • light-induced Ca^{2+} fluxes • Ca^{2+} source function • intracellular Ca^{2+} concentration

INTRODUCTION

In the dark, an Na^+ current circulates between the inner and outer segment of the rod photoreceptor (Hagins et al., 1970; Penn and Hagins, 1972). This dark current is generated in the inner segment by means of an Na^+/K^+ ATPase. From the inner segment the dark current flows extracellularly to the outer segment, entering the rod again via cGMP-dependent ion channels. Light absorption by rhodopsin initiates a reduction of the dark current: Activated rhodopsin (R*)[1] causes a G-protein–mediated stimulation of a cGMP-specific phosphodiesterase (PDE) leading to an enhanced hydrolysis of cGMP. As a consequence, the free cGMP concentration in the outer segment falls. Thus, the cGMP-dependent ion channels close so that the Na^+ influx into the outer segment decreases (for review see Pugh and Lamb, 1990).

In addition to the Na^+ influx a remarkable flow of Ca^{2+} ions into the outer segment is observed through the light-regulated ion channels (Hodgkin et al., 1985; Nakatani and Yau, 1988). In the dark, the Ca^{2+} influx is balanced by a Ca^{2+} efflux from the outer segment via an Na^+/K^+–Ca^{2+} exchanger (Yau and Nakatani, 1985; Cervetto et al., 1989; Friedel et al., 1991). A light-induced closure of the cGMP-dependent ion channels also reduces the Ca^{2+} influx into the outer segment. Thus, after light stimulation, a net Ca^{2+} efflux remains so that the Ca^{2+}concentration is increased in the extracellular medium (Yoshikami et al., 1980; Gold, 1986; Cieslik and Rüppel, 1988) but reduced in the outer segment (Yau and Nakatani, 1985; Gold, 1986; Miller and Korenbrot, 1987; Ratto et al., 1988).

In amphibian rods, the reduction of the Ca^{2+} concentration in the outer segment after a flash of light accelerates the restoration of the dropped cGMP concentration to the dark level (Koch and Stryer, 1988; Yau and Nakatani, 1988; Matthews, 1991) and causes an adaptation to steady background light (Matthews et al., 1988). Both effects can be explained by a stimulated activity of a guanylate cyclase (GC) that resynthesizes cGMP (Koch and Stryer, 1988). Since the GC is known to be inhibited by Ca^{2+} ions, the cGMP synthesis becomes activated if the Ca^{2+} concentration in the outer

Address correspondence and reprint requests to Prof. H. Rüppel, Max Volmer Institut PC 14, Technische Universität Berlin, Str. des 17. Juni 135, D-10623 Berlin, Germany.

[1] *Abbreviations used in this paper:* GC, guanylate cyclase; LED, light-emitting diode; PDE, phosphodiesterase; R/R*, rhodopsin/activated rhodopsin; ros, rod outer segment.

 J. GEN. PHYSIOL. © The Rockefeller University Press • 0022-1295/96/05/577/19 $2.00
Volume 107 May 1996 577–595

segment is reduced. However, the action of Ca^{2+} on the transduction pathway seems to be more complex: Ca^{2+} ions are also reported to effect the rhodopsin deactivation (Wagner et al., 1989; Knopp and Rüppel, 1993; Kawamura, 1993; Knopp, 1994), to reduce the R*/PDE gain (Pepperberg et al., 1994; Lagnado and Baylor, 1994), and to interact with the cGMP-dependent ion channels from the cytoplasmatic side (Hsu and Molday, 1993).

Because of the various interactions of Ca^{2+}, it is important to know how light alters the Ca^{2+} concentration and the Ca^{2+} fluxes in the outer segment. Under physiological conditions, the Ca^{2+} concentration in the outer segment can be directly measured solely during completely interrupted dark current (Ratto et al., 1988). Until now the Ca^{2+} efflux was mainly determined by the measurement of the Ca^{2+} exchange current in amphibian rods using suction electrodes (Hodgkin et al., 1987; Yau and Nakatani, 1988; Yau and Nakatani, 1985; Nakatani and Yau, 1988). With mammalian rods, only one detailed study about the Ca^{2+} efflux was performed by these suction electrodes (Tamura et al., 1991). As the Ca^{2+} exchange current is obtained during complete interruption of the dark current only, the method does not allow for the observation of the Ca^{2+}exchange current after stimulation by dim flashes and during the time period of the dark current regeneration.

In a few studies of amphibian rods, Ca^{2+}-selective electrodes were used to derive the Ca^{2+} fluxes from measurements of the extracellular Ca^{2+} concentration. (Gold, 1986; Miller and Korenbrot, 1987). However, since differences between amphibian and mammalian rods are suggested (Pugh and Altmann, 1988), the results from amphibian rods may not be assigned to mammalian rods. Only one unique determination of the Ca^{2+} efflux from mammalian rods was performed by use of Ca^{2+}-selective electrodes (Yoshikami et al., 1980). However, in this study only one dim flash intensity was used. Moreover, a disadvantage of all these methods used until now is that a uniform distribution of Ca^{2+} sources along the outer segment had to be assumed.

We here report on a special method to determine the Ca^{2+} fluxes through the rod plasma membrane from simultaneous measurements of the dark current and the Ca^{2+} concentration in the extracellular space of the photoreceptor layer. From the measured data, the net Ca^{2+} efflux is obtained by applying a specific, one-dimensional diffusion equation. In contrast to other approaches, the new method enables the Ca^{2+}fluxes to be determined even at distinct sites along the tiny mammalian rods. The method was used to study Ca^{2+} fluxes in rat rods during a photoresponse and to determine the time course of the free Ca^{2+} concentration in the rod outer segment. Our results mainly agree with earlier findings obtained from amphibian rods. It is shown that light causes the outer segment to be the main Ca^{2+}source. However, unexpectedly, only a part of the Ca^{2+} extruded from the outer segment during a photoresponse is restored, and a permanent Ca^{2+}efflux from the outer segment during steady light is obtained. The results are discussed in terms of Ca^{2+} fluxes that may be present in the rod.

MATERIALS AND METHODS

Materials

Albino Wistar rats were obtained from Schering AG (Berlin, Germany). The Ca^{2+}-selective liquid membrane (Ca-Cocktail A), carbontetrachloride (CCl_4), tetrahydrofurane, and trimethylchlorosilane (Me_3SiCl) were purchased from Fluka (Neu Ulm, Germany).

Incubation Medium and Retinal Preparation

Ringer's solution was prepared after Hagins et al. (1970) consisting of 130 mM NaCl, 2.2 mM KCl, 0.18 mM Mg · 6 H_2O, 11 mM glucose, 1.3 mM KH_2PO_4, 5.4 mM Na_2HPO_4, and 10 mM HEPES. The solution was titrated to pH 7.4 by NaOH. The final Ca^{2+} concentration was adjusted by adding appropriate amounts of a $CaCl_2$ stock solution.

Albino rats were kept in complete darkness for 2 h or more before they were killed by peritoneal injection of 2 ml of the Na^+ pentobarbitural (Nembutal®, Ceva AG, Bad Segeberg, Germany). After cardial arrest, the eyes were enucleated and the bulbus was cut in the meridian into two halves. The lower eye cup containing the retina was transferred into Ringer's solution. After ~10 min, the retina was gently removed from the pigment epithelium and was stored in Ringer's solution at room temperature in darkness. For recordings, pieces of ~1 mm^2 of the retina were placed receptor side up on a cellulose acetate filter (SM 11104; Satorius, Göttingen, Germany) and transferred into the recording chamber. The preparation was carried out under dim red light.

Recording Chamber and Photostimulation

The recording chamber (Fig. 1) consisted of a glass cuvette filled with Ringer's solution and grounded by an Ag/AgCl wire. The cuvette was embedded in a black anodized aluminium block, which was thermostated by a Peltier element. The perfusion of the recording chamber with Ringer's solution was driven by gravitation. The perfusate was collected by suction.

The illumination of the piece of retina within the recording chamber was achieved from below the chamber using flashes produced by a pulsed LED (Rüppel et al., 1978) or steady light via a splitted waveguide. The light intensity was attenuated by neutral density filters (No. 96; Eastman Kodak Co., Rochester, NY).

Electrode Preparation and Recording Assembly

From above the recording chamber, a double-barreled recording microelectrode (1, 2) was moved into the retina between the photoreceptor cells (cf. Fig. 1). This was performed by of a stepper motor (AM2 M2; Bachofer, Reutlingen, Germany) with a

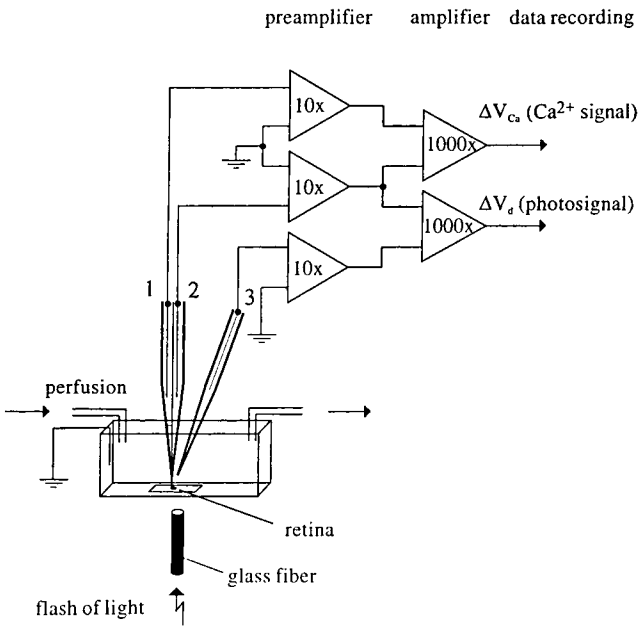

FIGURE 1. Schematic representation of the measuring device with flow chamber and assembly of double- and single-barreled electrodes. By the Ca^{2+}-sensitive barrel (*1*), the Ca^{2+} concentration is detected, whereas the voltage-sensitive barrel (*2*) measures simultaneously a voltage produced by the dark current in the extracellular space between the rods. The reference electrode (*3*) is positioned at the rod tips of the retinal layer. The arrangement of difference amplifiers directly yields output voltages that are dependent on changes of the Ca^{2+} concentration (*Ca^{2+} signal*) and the extracellular potential (*photosignal*).

step precision of ±0.15 μm. A second microelectrode located ~100 μm above the retina was used as a reference electrode (3).

One barrel of the recording electrode was filled with Ringer's solution (2). The other barrel (1) was prepared as a Ca^{2+}-selective microelectrode. For this purpose, it was filled with a solution of 10 mM $CaCl_2$ and 135 mM KCl. The tip of this barrel was then silanized by sucking a solution of CCl_4/Me_3SiCl into the tip. Subsequently, by weak suction, the silanized barrel tip was filled with Ca-Cocktail A. The reference electrode was pulled to a tip diameter of ~1 μm and filled with Ringer's solution, also. The double-barrel microelectrodes showed a tip diameter of 1.5–3.0 μm. After preparation, all microelectrodes were provided with an Ag/AgCl wire.

The resistance of the Ca^{2+}-selective barrel amounted to 5–10 GΩ. The voltage sensitive barrel and the reference microelectrode showed resistances of 4–8 MΩ. The Ca^{2+}-selective microelectrodes were selected for the measurements if they revealed a rise time 50–80 ms and a steepness of 27–30 mV per decade. The latter was determined with test solutions containing 0.1–1 mM $CaCl_2$ and 150 mM NaCl.

Voltage signals were recorded by a difference amplifier of high-input impedance (Neuro Hel IRIS; Meyer, München, Germany) and further amplified by a cascade of difference amplifiers with RC low-pass filters. The overall transmission band was 13 Hz. The amplifier assembly enabled the separation of the different voltage components of the recording electrode: the Ca^{2+} signal, i.e., a change of the extracellular Ca^{2+} concentration, and the photosignal, i.e., a potential difference derived from changes in the dark current (see Fig. 1).

The entire measuring and recording equipment was completely placed inside a Farady box.

Measuring Procedure for Determination of the Net Ca^{2+} Efflux

Beginning usually 40 μm above the retina, the tip of the electrode was moved towards and into the retina by steps of Δz_0 = 8 μm. The tip area of the outer segments was adjusted to $z = 0$ (cf. Fig. 2). At each position z of the measuring electrode, the retina was stimulated by light and the changes of the extracellular Ca^{2+} concentration (Ca^{2+} signal) as well as the potential differences caused by the light stimulation (photosignal) were recorded as a function of the time t after the onset of light (see Fig. 5). As a rule, averages of two to three signals were taken. The data set representing the complete space and time dependence of the concentration changes is sufficient to calculate the appearance of Ca^{2+} sources and sinks (source function q (z, t)) at any position z along the rod and the time t after the onset of light stimulation.

As the cross-section of the tip of the double-barrel electrode (2–7 μm^2) is usually larger than the free interstitial space of the retina (~1 μm^2, see below), the question of whether the retina is not damaged by the electrode insertion procedure must be raised. Otherwise, both receptor signals might be subject to distortion. Furthermore, during long-time data collection, the aging of the isolated retina, which is detectable by the run-down of the

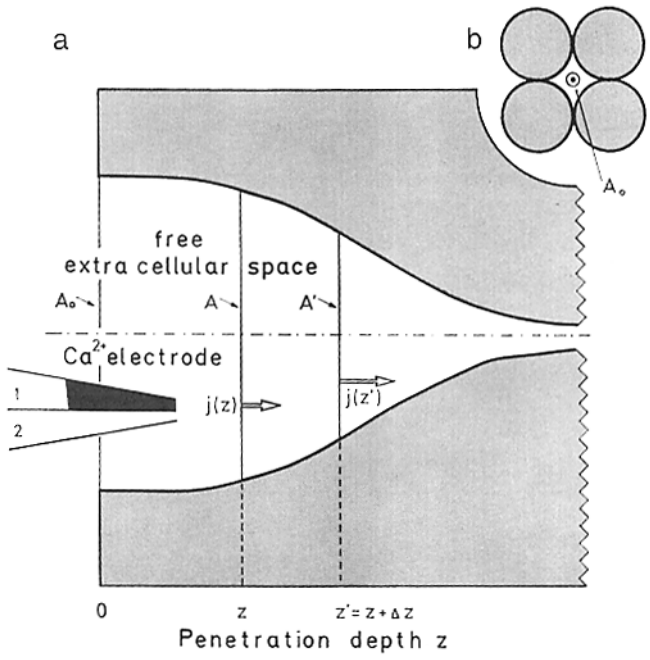

FIGURE 2. Schematic representation of the free extracellular space between the rods. (*a*) Axial view showing the change in cross-section area versus penetration depth z. (*b*) Cross-section of a rod array at the tip of outer segment ($z = 0$). A_0, A, A': cross-section areas at different penetration depths 0, z, z'.

rod dark current, had to be considered. This was especially important if the retina was successively stimulated by steady light. In this case, several minutes of intermission were allowed in between to ensure a complete regeneration of the retina back to the dark state. Thus, the total measuring time added up to at least 30 min. With respect to retinal stability during this measuring period, the results of earlier long-time studies of the isolated rat retina in the course of electrode insertion could be used for reference. These studies revealed a half-life of the retina between 50 and 500 min (Kuhls et al., 1995). With respect to possible retina damage during electrode insertion, however, thorough bracketing measurements performed by Hagins et al. (1970) show that there is no hysteresis in the dark voltage trace between insertion and withdrawal of the electrode in a rat retina. To prove whether this observation applies also to the recording of the Ca^{2+} concentration, particular control measurements were performed. One example is shown in Fig. 3. The maximum amplitude value as well as the half-rise time of Ca^{2+} signals are plotted versus the penetration depth z. The signals with numbers N = 1–13 were recorded during the insertion of the electrode from above the retina ($z = -48$ μM) deeply down into the nuclear layer ($z = -56$ μM), whereas the Ca^{2+} signal $N = 14$ was evoked during the withdrawal at $z = 8$ μM, i.e, at the most sensitive location of maximum amplitude. The amplitude value and the half-rise time of the control signal ($N = 14$) fit perfectly to the set of signal data measured at neighboring positions. This would not be the case if retinal damage caused by the electrode insertion as well as a significant run-down of the receptor current had taken place during this experiment. Therefore, the control measurement shows that the procedure of electrode insertion yields reversible results.

Theory

Ca^{2+} ion diffusion in the extracellular space. Light-induced changes of Ca^{2+} concentration are measured in the extracellular space of the retinal rod layer (see Fig. 2). These concentration changes result from Ca^{2+} transport processes across the plasma membrane of the rods and diffusion processes outside the rods. The extracellular space is defined by the lateral arrangement of the closely packed rods, which on the average can be represented by a quadratic lattice. Thus, it is evident that the outer space in between four rods shows an axial symmetry with respect to a longitudinal axis (see cross-section in Fig. 2). The Ca^{2+} transport processes in this outer space are described by the diffusion equation

$$\frac{\partial c}{\partial t} + div\, j = q\,(x,y,z;t) \qquad (1)$$

which in cylindrical coordinates is given by

$$\frac{\partial c}{\partial t} - D\left(\frac{\partial^2 c}{\partial z^2} + \frac{1}{r^2}\,\frac{\partial^2 c}{\partial \Phi^2} + \frac{1}{r}\,\frac{\partial}{\partial r} r \frac{\partial c}{\partial r}\right) = q\,(z,r,\Phi;t)\,, \qquad (2)$$

where z denotes the longitudinal axis, i.e., the direction of electrode penetration, c is the Ca^{2+} concentration in the extracellular space, $j = -D \cdot \text{grad}\ c$, the Ca^{2+} flux density, D is the diffusion constant for Ca^{2+} ions, and $q(z,r,\Phi,t)$ is the source function for which the time-dependent sources and sinks are localized at the boundaries of the extracellular space, i.e., the rod surfaces.

As the radial distances between the rods are much smaller than the longitudinal pathway for the Ca^{2+} ion flux, the equilibration of concentration gradients proceeds much faster in the radial than the axial direction. Thus, in a first approximation, for any cross-section area $A(z)$, the radial concentration gradient $(\partial c/\partial r)_z$ as well as the circumferential gradient $(\partial c/\partial \Phi)_z$ should be zero so that the two lateral terms in Eq. 1 could be neglected. Even under the assumption of diminishing lateral gradients, however, a radial flow of Ca^{2+} ions must be considered if the cross-section area alters in axial direction, i.e., for $\partial A/\partial z \neq 0$. This radial flow results in a considerable contribution to the source function, which has to be allowed for if the net Ca^{2+} flux across the rod plasma membrane is being determined. In fact, the actual source function can be derived from the divergence of the axial Ca^{2+} ion flux if changes in the cross-section area are taken into account: For an axial flow of Ca^{2+} ions

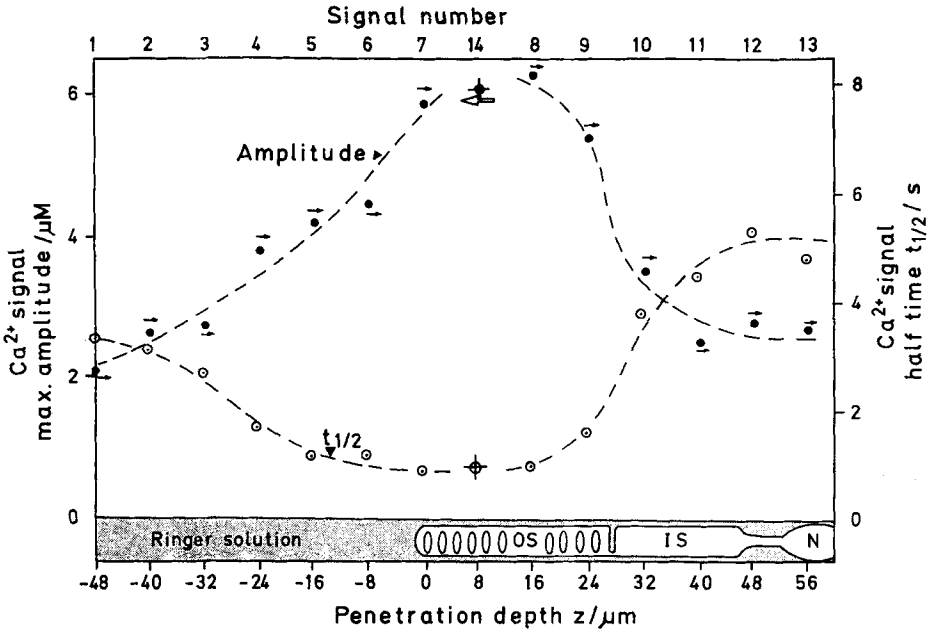

FIGURE 3. Maximum amplitude (●) and half-rise time $t_{1/2}$ (⊙) of Ca^{2+} signals measured at different positions $z = -48$ μm to $+56$ μm while inserting the double-barreled electrode into the rod layer of a rat retina (signal No. 1–13) The rod tips were positioned at $z = 0$. The retina was stimulated by steady light of saturating intensity of 10 s duration. The time period between each singular measurement was 3 min. Regular step width was 8 μm. The signal at position $z = 8$ μm (No. 14) was recorded after the electrode was withdrawn from the inner nuclear layer. Amplitude and rise time of signal No. 14 (-●- and ⊕) fit well with the Ca^{2+} signal data obtained during electrode insertion at neighboring positions.

$$j(z) = -D\frac{\partial c}{\partial z}(z),$$

the divergence within a space interval between z and $z' = z + \Delta z$ and boundary areas A and $A' = A + \Delta A$ is approximated by

$$\begin{aligned} div\, j(z) &= \frac{A' \cdot j(z') - A \cdot j(z)}{\overline{\Delta V}} \\ &= -\frac{(A + \Delta A) D\frac{\partial c}{\partial z}(z + \Delta z) - A \cdot D\frac{\partial c}{\partial z}(z)}{\overline{A} \cdot \Delta z} \\ &= -D\frac{A}{\overline{A}}\left(\frac{\frac{\partial c}{\partial z}(z + \Delta z) - \frac{\partial c}{\partial z}(z)}{\Delta z}\right) \\ &\quad -\frac{D}{\overline{A}} \cdot \frac{\Delta A}{\Delta z}\,\frac{\partial c}{\partial z}(z + \Delta z), \end{aligned} \tag{3}$$

where $\overline{\Delta V} = \overline{A} \cdot \Delta z\,[\overline{A} = (A + A')/2]$ is the average volume (cf. Fig. 2). In the limit $\Delta z \to 0 (\overline{A} \to A)$, the divergence follows as

$$\begin{aligned} div\, j &= -\lim_{\Delta z \to 0}\left[\left(D\frac{A}{\overline{A}}\,\frac{\frac{\partial c}{\partial z}(z + \Delta z) - \frac{\partial c}{\partial z}(z)}{\Delta z}\right)\right. \\ &\quad \left. -\frac{D}{\overline{A}}\,\frac{\Delta A}{\Delta z}\,\frac{\partial c}{\partial z}(z + \Delta z)\right] \\ &= -D\frac{\partial^2 c}{\partial z^2} - D\frac{1}{A}\,\frac{dA}{dz}\,\frac{\partial c}{\partial z}. \end{aligned}$$

Thus, according to Eq. 1, a one-dimensional differential equation

$$\frac{\partial c}{\partial t} - D\left(\frac{\partial^2 c}{\partial z^2} + \frac{1}{A}\,\frac{dA}{dz}\,\frac{\partial c}{\partial z}\right) = q(z,t) \tag{4}$$

is obtained that sufficiently describes the extracellular Ca^+ transport processes within the rod layer. The additional diffusion term in Eq. 4 showing a first-order derivation of concentration depends on the relative change in the cross-section area of the extracellular space and corresponds to the radial Ca^{2+} flow. As there is a drastic area change, indeed, between the outer and inner segment of the rod (see below), this term cannot be neglected and must be deduced from the partial concentration change $(\partial c/\partial t)_z$ to obtain the actual source function $q(z,t)$ along the surface of the rod.

Numerical calculation of the source function. For a numerical calculation of the source function, a simple difference equation was derived from Eq. 3 as follows: The measurements with microelectrodes were performed in equidistant positions along the rod axis. If the constant step width is Δz_0 (= 8 μm), Eq. 3 can be rewritten for these discrete intervals $\Delta z = \Delta z_0$ as

$$\begin{aligned} div\, j(z) \approx -D\Big(A'\frac{c(z + \Delta z_0) - c(z_0)}{\Delta z_0} \\ -A\frac{c(z_0) - c(z - \Delta z_0)}{\Delta z_0}\Big) \Big/ (A\Delta z_0). \end{aligned}$$

According to Eq. 1, the source function $q(z,t)$ is approximated by

$$\begin{aligned} q(z,t) \approx \frac{\Delta c}{\Delta t} - \frac{2D}{\Delta z_0 (A' + A)} \cdot \Big(A'\frac{c(z + \Delta z_0) - c(z_0)}{\Delta z_0} \\ -A\frac{c(z) - c(z - \Delta z_0)}{\Delta z_0}\Big). \end{aligned} \tag{5}$$

Eq. 5 is used to calculate the source function from the measured data.

Determination of cross-section A(z) in the extracellular space. The cross-section area was estimated as follows: At the tip of the outer segment at $z = 0$, the area $A(o)$ was estimated by assuming an arrangement of rods within a quadratic lattice. If the rods occupy the lattice points, the lattice constant is $2r$ (r = radius of outer segment) and the cross-section area of the free space between the rods is $A(o) = (4 - \Pi)r^2$. In the case of the rat, one has r = 0.9 μm (Hagins et al., 1970) and consequently $A(o)$ = 0.70 μm². Nearly the same value (exactly 0.74 μm²) was measured by us for the free interstitial space from a transmission electron micrograph taken by Hagins (1973, unpublished) showing a lateral cut through the rod outer segment layer of a rat retina.

The alteration of $A(z)$ with increasing $z > 0$ is shown in Table I.

TABLE I

A.	*Relative Cross-Section Area of Free Extracellular Space*										
z/μm	0	4	12	20	28	36	44	52	60	68	76
A(z)/A(o)	1	0.99	0.96	0.84	0.60	0.33	0.17	0.15	0.14	0.13	0.13

B.	*Smoothing Equations for Signal Amplitudes* $A(z_n, t_n)$
1.	$A^s_{n-2} = 1/70 \cdot (69\,A_{n-2} + 4\,A_{n-1} - 6\,An + 4\,A_{n+1} - 1\,A_{n+2})$
2.	$A^s_{n-1} = 2/70 \cdot (2\,A_{n-2} + 27\,A_{n-1} + 12\,An - 8\,A_{n+1} + 2\,A_{n+2})$
3.	$A^s_n = 2/70 \cdot (-3\,A_{n-2} + 12\,A_{n-1} + 17\,An + 12\,A_{n+1} + 3\,A_{n+2})$
4.	$A^s_{n+1} = 2/70 \cdot (2\,A_{n-2} - 8\,A_{n-1} + 12\,An + 27\,A_{n+1} + 2\,A_{n+2})$
5.	$A^s_{n+2} = 1/70 \cdot (-1\,A_{n-2} + 4\,A_{n-1} - 6\,An + 4\,A_{n+1} + 69\,A_{n+2})$

(*A*) The relative cross-section area of the free extracellular space in dependence of the penetration depth z was derived from the longitudinal resistance R_z per unit length as measured by Hagins et al. (1970) within the isolated life rat retina. The longitudinal resistance is inversely proportional to $A(z)$ so that $A(z) = [R_z(o)/R_z(z)] \cdot A(o)$. (*B*) For data smoothing, an algorithm reported by Allen and Tildesley (1987) was used. A_n denotes data values before, A^s_n after applying a smoothing operation. Eqs. 1 and 2 are applied to obtain the first and second, whereas Eq. 4 and 5 are applied to yield the last two of the smoothed values. Eq. 3 was used to smooth the other values of the data set. The smoothing operation was applied alternatingly three times each in space and time. The step width was Δz_0 = 8 mm and Δt_0 = 30 ms.

The data of the cross-section area $A(z)$ is derived from the longitudinal resistance per unit length

$$R_z = \frac{dR}{dz}$$

of the extracellular space as measured by Hagins (Hagins et al., 1970): The longitudinal resistance is inversely proportional to $A(z)$ so that

$$A(z) = [R_z(o)/R_z(z)] \cdot A(o).$$

Calculation of net transmembrane Ca^{2+} fluxes. The net efflux of Ca^{2+} ions from the rod [1/s] into the adjacent infinitesimal volume element $dV = A(z)dz$ is derived from the source function $q(z,t)$ [M/s] by

$$dQ(z,t) = q(z,t) \cdot N_A^{-1} \cdot A(z)\,dz$$

or per unit length as

$$\frac{dQ(z,t)}{dz} = q(z,t) \cdot N_A^{-1} \cdot A(z), \tag{6}$$

where N_A is Avogadro's constant.

Consequently, the total net Ca^{2+} efflux $Q(z,t)$ between the position z_0 and z is obtained by the axial integral

$$Q(z,t) = \int_{z_0}^{z} Q_z(z,t)\,dz = \int_{z_0}^{z} q(z,t) \cdot A(z) \cdot N_A^{-1}\,dz.$$

Thus, the net Ca^{2+} outflow $Q_{OS}(t)$ from the whole outer segment, i.e., between $z_0 = 0$ and $z_i = 25$ μm is given by

$$Q_{os}(t) = \int_{z_0}^{z_i} Q_z dz = \int_{0}^{25\mu} q(z,t) \cdot N_A^{-1} A(z) dz. \tag{7}$$

The amount of Ca^{2+} ions that is pumped out of the rod plasma membrane at the position z into the space volume element $dV = Adz$ between $t = 0$ (time of light onset) and the time t after light onset is given by

$$\Delta Ca_z = \int_0^t Q_z(t)\,dt. \tag{8}$$

Finally, the total amount of Ca^{2+} extruded from the whole outer segment at the time t after light onset is

$$\Delta Ca_{os} = \int_0^t Q_{os}(t)\,dt. \tag{9}$$

In practice, the integral $Q_{OS}(t)$ of Eq. 6 can be approximated by a sum

$$Q_{os} \approx \sum_{i=1}^{3} \Delta Q(z_i) = \left(\sum_{i=1}^{3} q_{z_i} A_{z_i} \right) \cdot N_A^{-1} \cdot \Delta z_0$$

$$= \left((qA)_{4\mu} + (qA)_{12\mu} + (qA)_{20\mu} \right) \cdot N_A^{-1} \cdot \Delta z_0 \tag{10}$$

where A_{z_i} is the mean value of the cross-section area between z_i and $z_i + \Delta z_0$.

Data smoothing. For the numerical calculation of the source function according to Eq. 4, the data of the Ca^{2+} measurements were smoothed by use of an algorithm reported by Allen and Tildesley (1987), which is given in Table I. This algorithm was originally developed for one independent variable only. For this calculation, however, the data smoothing procedure was applied $n = 3$ times alternatingly in time t and penetration depth z. The sample interval was $\Delta z_0 = 8$ μm in z and $\Delta t_0 = 30$ ms in t. The smoothing operation was extended over two intervals on each side of the sample point (see Table I). For each run, a limitation in the signal bandwidth in space or in time occurs that can be approximated by a linear integration step over $m = 3$ sample intervals. For a single application of the smoothing algorithm according to Shannon's theorem, the bandwidth of the signal presentation is limited to $\Delta f = (2 \cdot m \cdot \Delta t_0)^{-1}$ in the t-axis and to $\Delta \tilde{f} = (2 \cdot m \cdot z_0)^{-1}$ in the z-axis (f = "time" frequency, $\tilde{f}$ = "space" frequency, Rüppel, 1983). An n-times repetition of this procedure corresponds to a series connection of n equal band path filters with a time or space constant of $\tau_B \approx \Delta t_0$ and $\lambda_B \approx \Delta z_0$, respectively. Finally, an alternating application of the smoothing procedure in time and space yields the product of both bandwidth reduction factors. Thus, in this particular case,

$$\Delta v^s = (2^{1/n} - 1) \cdot m^{-2} \cdot \Delta v_0 = 0.4 \text{ Hz},$$

which corresponds to a rise time of 0.9 s for $\Delta v_0 = 13$ Hz; $n = 3$, $m = 3$.

RESULTS

Changes of Extracellular Ca^{2+} Concentration after Flashes of Light

Flash-induced changes of the extracellular Ca^{2+} concentration were measured in the extracellular space. Fig. 4 represents Ca^{2+} changes $\Delta[Ca]_o$ recorded at different retinal depths z in dependence of the time t after a saturating flash that completely interrupted the dark current for ~1.5 s. The Ca^{2+} signals are plotted in a three-dimensional $\Delta[Ca]_o(z,t)$ representation and are shown for four different values of the extracellular Ca^{2+} concentration: (*a*) 0.1, (*b*) 0.2, (*c*) 0.5, and (*d*) 1 mM. First of all, it is conspicuous that the time courses of the Ca^{2+} concentration changes $\Delta[Ca]_o$ depend on the penetration depth z of the electrode. Near the outer segment (z = 0–25 μm), after flash stimulation, the Ca^{2+} concentration increases with maximum rate and maximum amplitude at all four Ca^{2+} concentrations in the Ringer's solution (see Fig. 4 *a–d*). The amplitude of the Ca^{2+} signal depends on the extracellular Ca^{2+} concentration. With the same flash strength, a maximum amplitude of 5 and 10 μM is produced if Ringer's solution contains 0.1 and 1 mM Ca^{2+}, respectively. The time course of the Ca^{2+} signals measured near the outer segment is independent of the Ca^{2+} concentration in the Ringer's solution. These observations suggest, first, that the outer segment acts as the main Ca^{2+} source for the light-induced increase of the extracellular Ca^{2+} concentration, and second, that the rate of the flash-induced Ca^{2+} release from the outer segment rises with the external Ca^{2+} concentration.

The Ca^{2+} signals recorded in Ringer's solution above the retina ($z < 0$) are smaller in amplitude and show a delayed maximum compared with Ca^{2+} signals recorded next to the outer segment. The difference Δt_p of the time to peak between a Ca^{2+} signal recorded within the outer segment layer and a Ca^{2+} signal recorded above the retina can be exactly described by the Einstein-Smoluchowski equation $\Delta t_p = 1/2 \cdot \Delta z^2/D$, where Δz is the distance between the leading electrode tip and

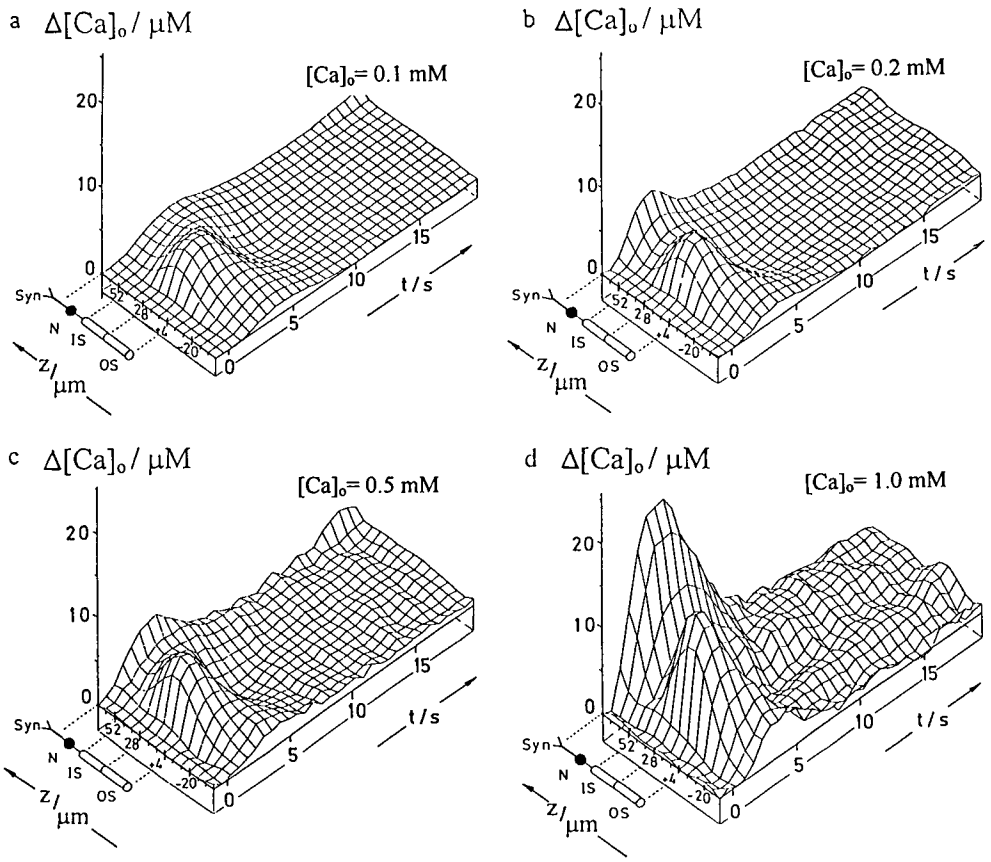

FIGURE 4. Three-dimensional representation of flash-induced changes in the extracellular Ca^{2+} concentration $\Delta[Ca]_o$ as a function of electrode position z and time t after the flash. The Ca^{2+} concentration of Ringer's solution was varied (in μM) as: (*a*) 100, (*b*) 200, (*c*) 500, (*d*) 1,000. The saturating flash was applied at $t = 0$ exciting 500R*/ros. The temperature was 30°C.

the center of the outer segment and D is the diffusion coefficient of Ca^{2+} in Ringer's solution (D = 1,000 $\mu m^2/s$, Yoshikami et al., 1980; Rüppel and Cieslik, 1988). Therefore, the elevation of the Ca^{2+} concentration above the retina can be attributed to Ca^{2+} ions that diffuse into the Ringer's solution after being released from the outer segments. This again proves the outer segment to represent the main Ca^{2+} source after flash illumination.

After passing a maximum, the elevated Ca^{2+} concentration starts to return to the dark level again. The most rapid decline is observed near the outer segments. In most of the experiments, the Ca^{2+} concentration between the outer segments transiently falls even below the dark level (see also Fig. 5 *b*). This indicates that, at the end of a photoresponse, the function of the outer segment reverses from the main Ca^{2+} source to the main Ca^{2+} sink.

Occasionally, at the synapses ($z \approx 60$ μm) a strong and rapid flash-induced increase of the extracellular Ca^{2+} concentration was observed. As a rule, however, it was difficult to investigate the origin of this phenomenon. For this purpose a very stable retina was necessary. The retina from which the Ca^{2+} signals shown in Fig. 4 were derived was such a stable one. From this particular retina, Ca^{2+} signals could be repeatedly recorded down to the synaptic region. Furthermore, the retina did not show a remarkable run-down during data collection and solution exchange. In this case the Ca^{2+} increase near the synapse was strong and rapid and depended considerably on the external Ca^{2+} concentration. At $[Ca]_o$ = 1,000 mM, the Ca^{2+} increase at the synapses even exceeded that measured at the outer segments (see Fig. 4 *d*), but it was much more attenuated at lower Ca^{2+} levels (see Fig. 4, *a–c*). However, with regard to Ca^{2+} fluxes, this increase should not be overestimated. The intercellular space in the synaptic region is very small, so that even small Ca^{2+} fluxes may cause a dramatic change of the Ca^{2+} concentration. As shown in Fig. 4, *a–d*, there is a reduced and delayed increase of the extracellular Ca^{2+} concentration between the outer segment and the synaptic region. Therefore, the increased Ca^{2+} concentration near the synapse is not due to a diffusion of Ca^{2+} ions from the outer segment to the synapse. The origin of the increasing extracellular Ca^{2+} concentration at the synapses is still unclear. This difficulty is mainly due to the limited number of stable retinae available. Thus, the problem of Ca^{2+} fluxes in the synaptic region could not be studied sufficiently and in detail.

Photosignals and Ca^{2+} Signals Recorded in the Outer Segment Region at Different Flash Intensities

The dark current of a rod is measured as a potential difference between the voltage-sensitive barrel (Fig. 1, 2) of the measuring electrode and the reference electrode (Fig. 1, 3), i.e., across a resistance in the interstitial space. The circulating current of the rod passes the plasma membrane of the outer segment via light-sensitive membrane channels that regulate the current. A light-induced, transient closure of the channels decreases the membrane conductance so that the rod current is reduced. The current change, however, causes a drop of the potential difference between the monitoring electrodes and thus produces the photosignal (Penn and Hagins, 1969; Hagins et al., 1970; cf. Kuhls et al., 1995). Therefore, as a rule, the time course of the photosignal should be the same as that of the conductance change, and this should be the case independent of the electrode position. This is supported by the fact that, in contrast to the Ca^{2+} signals (see above), the time course of the photosignal does not depend on the penetration depth z. This was measured by Lamb et al. (1981) along the outer segment of detached rods. In fact, in this study a photosignal could be measured with high accuracy, i.e., with sufficient signal-to-noise ratio only beyond the outer segment region. That means, even in the case that in the intact retina the relative time course of current inflow is not the same at all positions z along the outer segment, the photosignal should represent the mean time course of the conductance changes in the outer segment membrane. Hence, the measured photosignal in the inner segment area was used to present the time course of the conductance and, correspondingly, the permeability for Na^+ and Ca^{2+} ions.

In principle, the space dependence and the time course of the outer membrane conductance can be derived also from the extracellular potential V. Measured by the amplitudes of saturated photosignals at different penetration depths, this extracellular potential $V(z)$ allows for the calculation of the sources and sinks of the receptor current.[2] Such an analysis of receptor currents was performed before by Penn and Hagins (1969) on the basis of photosignal measurements. As the potential gradient is due to other ion fluxes than Na^+ alone, this procedure is subject to considerable error (Cieslik and Rüppel, unpublished results). Therefore, in this study it seemed to be more convenient and reliable to take the mean time course of the membrane current directly from photosignals.

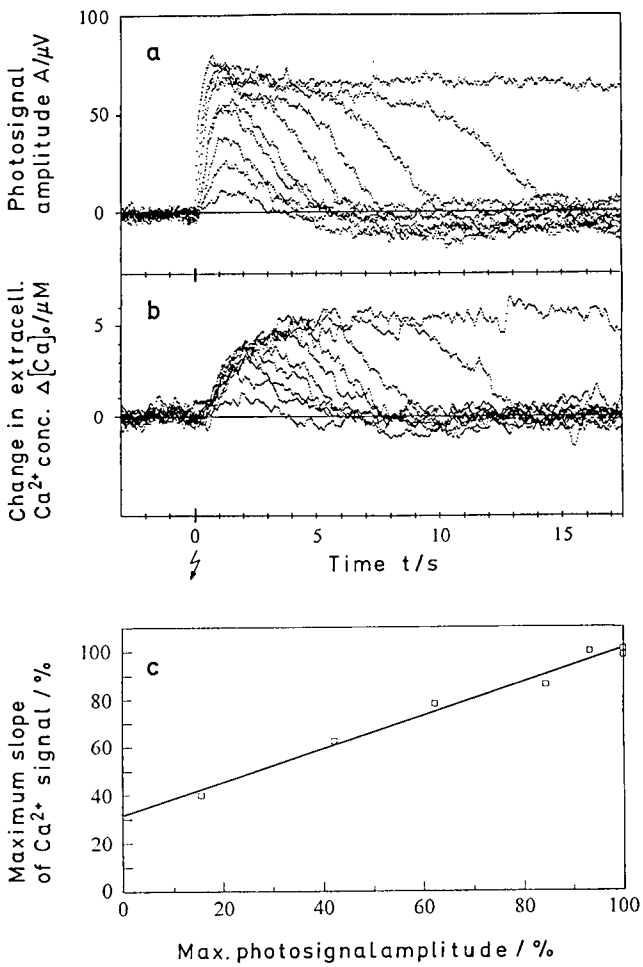

FIGURE 5. Result of a microelectrode measurement in a rat retina at an extracellular Ca^{2+} concentration $[Ca]_o$ = 250 μM and temperature of 22°C. The rat retina was penetrated by the recording electrode to z = 20 μm. (*a*) Photoresponse amplitude (photosignal) and (*b*) change in Ca^{2+} concentration (Ca^{2+} signal) after application of flashes at t = 0 exciting 7, 15, 30, 60, 120, 190, 380, 750, 3,800, and 38,000 R*/ros. (*c*) Maximum slope of the Ca^{2+} signal (see *b*) in dependence of the maximum amplitude of the corresponding photosignal.

Typical photosignals evoked by flashes of increasing strengths are shown in Fig. 5 *a*. As already shown in previous studies (Hagins et al., 1970; Penn and Hagins, 1972; Rüppel and Cieslik, 1989), weak flashes of up to 250 v/ros produce photosignals with distinct peak amplitudes that increase with flash strength by a hyperbolic function. More intense flashes saturate the photoresponse. These saturating photosignals show a plateau

[2] For evaluation, the charge transport equation that corresponds to the diffusion equation given by Eq. 1 must be applied. In this case, the Ca^{2+} concentration c is replaced by the charge density ρ, the Ca^{2+} flux density by the current density $j = -\kappa \cdot \text{grad } V$, and the diffusion constant by the ion conductivity κ. As for these relatively slow measurements (signal rise time > 0.1 s), all charging processes of membrane capacities are stationary; the partial derivate $(\partial\rho/\partial t)_z$ is zero everywhere. Therefore, the source function $q(z,t)$ (Eq. 1) is given by the divergence term in voltage only. Thus, the time course but not the amplitude of the source function should be independent of the penetration depth z.

phase during which the dark current is completely suppressed. Increasing strength of the saturating flashes prolongs the plateau phase of the photosignal.

In Fig. 5 *b*, Ca^{2+} signals that were recorded simultaneously with the photosignals shown in Fig. 5 *a* by means of the Ca^{2+}-sensitive barrel (1) of the leading electrode are shown. These Ca^{2+} signals were measured near the outer segment in response to flashes of increasing strength. Like the photosignals, the Ca^{2+} signals show a time course that is dependent on the flash strength. However, the time courses are obviously completely different: If nonsaturating flashes are applied, the extracellular Ca^{2+} concentration increases slowly and reaches a maximum amplitude shortly after the photosignal has passed its maximum. Enhancing the flash strength increases the initial slope rate and the maximum amplitude of the Ca^{2+} signal. If saturating flashes are applied, the Ca^{2+} concentration increases with a maximum initial slope along a common time course, reaching a maximum amplitude when the plateau phase of the photosignal is finished. During long-lasting plateau phases, the Ca^{2+} concentration between the outer segments reaches a constant maximum level (~5.5 μM in Fig. 5 *b*). At the end of the plateau phase, when the dark current begins to recover, the elevated Ca^{2+} concentration starts to return to the dark level again.

The diagram in Fig. 5 *c* represents the initial slope of the Ca^{2+} signal as a function of the maximum photosignal amplitude. Surprisingly, the Ca^{2+} concentration increases with an initial rate that is correlated by a linear function with the maximum of the photosignal. The reason for this remarkable relation is not known. However, it corroborates the evidence given above: When the dark current is completely suppressed by a saturating flash the external Ca^{2+} concentration, $[Ca]_o$ increases with a maximum initial slope (see Fig. 5 *b*). In the case of saturating flashes, the closure of the membrane channels occurs faster than the external Ca^{2+} concentration increases (at least six times, cf. Fig. 5, *a*

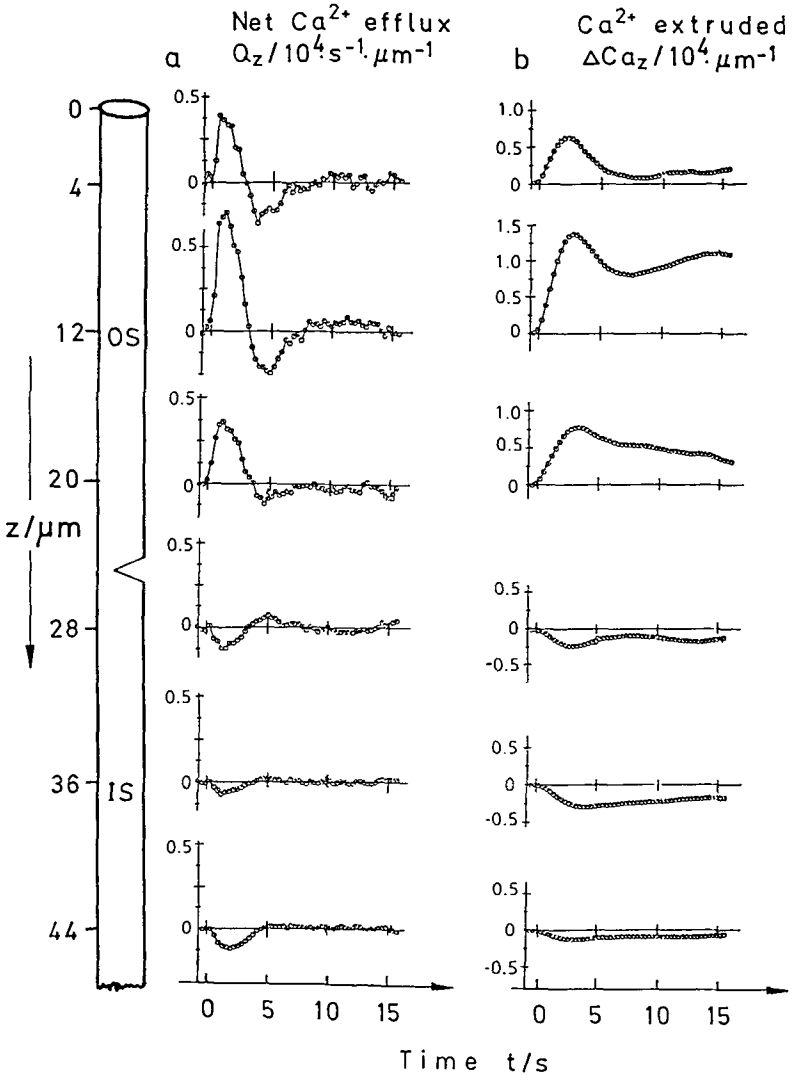

FIGURE 6. (*a*) Net Ca^{2+} efflux Q_z from the rod (per unit length) determined from the light-induced increment $\Delta[Ca_o]$ of the external Ca^{2+} concentration given at different electrode positions z (see Fig. 4). The retina was stimulated at $t = 0$ by a flash exciting 500 R*/ros. The temperature was 30°C. The Ringer's solution contained 200 μM Ca^{2+}. (*b*) Amount of Ca^{2+} ions ΔCa_z extruded from the rod (per unit length). ΔCa_z was obtained by integration of the corresponding Ca^{2+} efflux Q_z (*a*, left column) over the time *t*. Q_z and ΔCa_z are depicted as a function of time *t* after the flash.

and *b*), so that, after saturating flashes, the rate of Ca^{2+} increase is not diminished by any Ca^{2+} influx.

If small diffusion losses from the external space of the outer segment area are neglected, the initial rate of Ca^{2+} increase can be directly related to the initial rate of Ca^{2+} release from the outer segment, i.e., the net Ca^{2+} efflux Q_{OS}. In conclusion, Fig. 5 *c* indicates that, in any case, the initial net Ca^{2+} efflux Q_{OS} increases with the flash strength, yielding a maximum when the photosignal approaches saturation.

Ca^{2+} Sources at Distinct Positions along the Rod

From the time- and space-dependent changes of the extracellular Ca^{2+} concentration as presented in Fig. 4, the source function $q(z,t)$ was calculated as described under Theory in Materials and Methods (see above). Finally, $Q_z(z_i,t)$ was derived from the source function that represents the net Ca^{2+} efflux per unit length of the rod at each microelectrode position z_i and at any time t after the flash (cf. Eq. 6).

Fig. 6 *a* shows the time course of the net Ca^{2+} efflux $Q_z(z_i,t)$ in penetration depths between 4 and 44 μm, which in the following considerations is regarded as a measure for the source function. In Ringer's solution just above the retina ($z < 0$), the source function is found to remain zero after the flash (not shown), proving that the change of the Ca^{2+} concentration above the retina is solely attributed to diffusion. Along the outer segments, however, immediately after the flash, Ca^{2+} sources appear. After reopening of the Na^+ channels in the plasma membrane of the outer segments, the sources vanish again and sinks occur temporarily. Finally, the source function becomes zero again, i.e., the dark state is reestablished.

From the inner segment up to the synapse, only Ca^{2+} sinks are found to appear after the flash (in Fig. 6 *a*, shown up to a depth of 44 μm). These sinks are not sensitive to the Ca^{2+} channel blocker verapamil (not shown). The appearance of Ca^{2+} sinks at the synapse suggests that the dramatic increase of the Ca^{2+} concentration in the synaptical region as shown in Fig. 4 must be due to diffusion. However, as already pointed out, the increase is not due to a diffusion of Ca^{2+} ions from the outer segments to the synaptical region.

The time integral $\int Q_z(t)dt$ of the Ca^{2+} efflux yields the net amount of Ca^{2+} ions ΔC_z pumped out of the photoreceptor at a depth z during the time t after the onset of light stimulation. Fig. 6 *b* illustrates ΔCa_z as a function of time t after the flash determined at distinct penetration depths z. Along the outer segment, ΔCa_z reaches a maximum when the Na^+ channels start to reopen. The subsequent decline of ΔCa_z indicates that Ca^{2+} ions flow back into the outer segment. Whereas, at the tip, the same amount of Ca^{2+} pumped out during the photoresponse flows back after reopening of

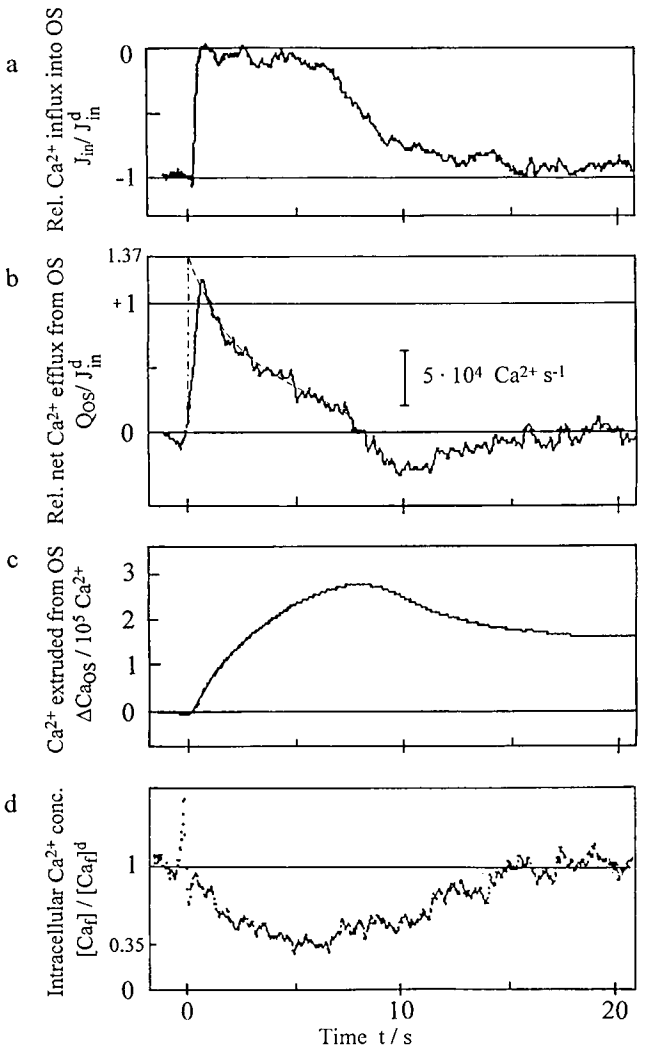

FIGURE 7. (*a*) Ca^{2+} influx into the outer segment, J_{in}, normalized to the dark value J_{in}^d. Since J_{in} is a constant fraction of the dark current, it is deduced from the photosignal by the equation $J_{in}/J_{in}^d = (A - A_{max})/A_{max}$, where A and A_{max} are amplitude and peak amplitude of the photosignal, respectively. The saturated photosignal was measured at a penetration depth $z = 28$ μm; (*b*) net Ca^{2+} efflux Q_{OS} from the outer segment normalized to J_{in}^d. (*c*) Net amount ΔCa_{OS} of Ca^{2+} ions extruded from the whole outer segment obtained by integration of Q_{OS} (trace *b*), and (*d*) time course of the intracellular Ca^{2+} concentration $[Ca^{2+}]_f$ normalized to the dark value $[Ca]_f^d$ derived from traces *a* and *b* as described in the Discussion. For calibration, it was presupposed that the initial value Q_0 of net efflux Q_{OS} is given by $Q_0 = \beta \cdot J_{eff}^d$. The activation factor $\beta = 1.37$ allows for the activation of the Na^+/K^+–Ca^{2+} exchanger. This activation is assumed to be caused by the hyperpolarization that follows the dark current shut-off after a saturating flash (Requena, 1983) and disappears again during dark current regeneration. As in the dark, one has $J_{in}^d = J_{eff}^d$, it follows $Q_0 = 1.37\, J_{in}^d$, which is used as calibration for Fig. 7 *d*. All traces *a*–*d* are plotted versus the time t after the flash. The retina was illuminated at $t = 0$ by a saturating flash exciting >250 R*/ros. The Ringer's solution contained 250 μM Ca^{2+}, the temperature was 23°C.

the Na^+ channels, surprising, only a part of it is restored in the middle and at the proximal end of the outer segment.

After the dark state is reestablished, the outer segment seems to have lost whereas the other compartments of the rod seem to have taken up a considerable amount of Ca^{2+} ions.

Net Ca^{2+} Efflux Q_{OS} from the Outer Segment

Fig. 7 *a* shows a photosignal derived at $z = 28$ μM after an intense flash of light that caused the dark current to be completely suppressed for ~7.5 s. As shown above, the time course of the circulating receptor current is sufficiently described by the photovoltage measured extracellularly. As a certain percentage of the inward membrane current is carried by Ca^{2+} ions (see below), the time course of the Ca^{2+} influx into the outer segment is represented directly by the time course of the photosignal. The corresponding net Ca^{2+} efflux Q_{OS} from the total outer segment after the flash is shown in Fig. 7 *b*. Q_{OS} is the axial integral $z_0\int^{z_i} Q_z\, dz$ between $z_0 = 0$ and $z_i = 25$ μm. The net Ca^{2+} efflux shown in Fig. 7 *b* reaches a maximum Q_{max} of $1.2 \cdot 10^5$ Ca^{2+}/s immediately after the flash. Subsequently, it declines exponentially with a time constant τ_Q of 4 s as long as the dark current is completely suppressed. At the moment the dark current begins to regenerate, the net efflux is followed by a temporary net influx indicating a restoration of Ca^{2+} ions in the depleted outer segment. Similar results were obtained from the rod of the toad *Bufo marinus* (Miller and Korenbrot, 1987) and from the bullfrog retina (Gold, 1986).

Fig. 7 *c* shows the amount ΔCa_{OS} of Ca^{2+} ions totally released from the whole outer segment up to the time *t* after the flash, which is obtained by time integration of Q_{OS} shown in Fig. 7 *b* as $\Delta Ca_{OS} = {}_0\int^t Q_{OS}\, dt$. A maximum of $2.8 \cdot 10^5$ Ca^{2+} are liberated from the outer segment during the photoresponse. However, only half of this amount is restored when the dark level is regained.

Fig. 7 *d* represents the corresponding time dependence of the intracellular Ca^{2+} concentration $[Ca]_f$, which was calculated as described in detail in the legend of Fig. 7 and in the Discussion. In principle, the time course of $[Ca]_f$ was derived from the Ca^{2+} efflux via the Na^+/K^+–Ca^{2+} exchanger, which is assumed to be proportional to $[Ca]_f$. The Ca^{2+} efflux, however, results from the difference between net Ca^{2+} efflux (trace 7 *b*) and Ca^{2+} influx (trace 7 *a*). Because of this procedure, the time course of $[Ca]_f$ is not directly related to ΔCa_{OS} as shown in Fig. 7 *c*. It is conspicuous that the internal Ca^{2+} concentration is found to return to the prestimulus dark level, although the extruded Ca^{2+} does not completely flow back into the outer segment. This surprising effect will be a subject of the Discussion.

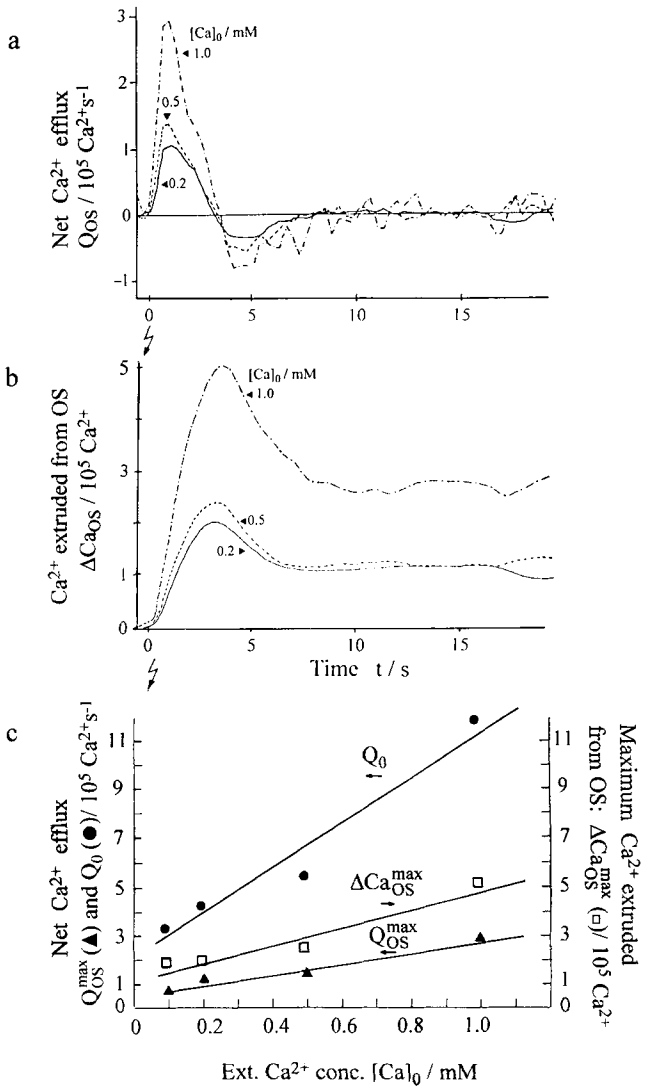

FIGURE 8. (*a*) Net Ca^{2+} efflux Q_{OS} from whole outer segment; (*b*) net amount of Ca^{2+} pumped out of the outer segment ΔCa_{OS}. The Ca^{2+} concentration was varied; the Ringer's solution contained 0.2 (—), 0.5 (····), 1.0 (- · -) mM Ca^{2+}. About 250 R*/ros were activated by the flash at $t = 0$. The temperature was 30°C, (*c*) Q_0, which is the extrapolated initial value of the net Ca^{2+} efflux (●), Q_{os}^{max}, which is the maximum of the net Ca^{2+} efflux (▲), and ΔCa_{os}^{max}, which is the peak value of Ca^{2+} ions extruded from the outer segment (□), are plotted in dependence of the extracellular Ca^{2+} concentration $[Ca]_o$. The data of diagram *c* were taken from *a* and *b*. The results of a measurement at 0.1 mM external Ca^{2+} concentration are not shown in *a* and *b* (for clarity) but are added in *c*.

Variation of the Ca^{2+} Concentration in Ringer's Solution

The net Ca^{2+} efflux Q_{OS} from the outer segment was determined for different concentrations in Ringer's solution by using the same piece of retina. Fig. 8 *a* shows the net Ca^{2+} efflux Q_{OS} as a function of time after the flash at 0.2, 0.5, and 1 mM Ca^{2+} in Ringer's solution. A fourth trace obtained at 0.1 mM was omitted in Fig. 8 *a*

for clarity. The magnitude of Q_{OS} increases with the external Ca^{2+} concentration in Ringer's solution. However, the time course of Q_{OS} is independent thereof.

Corresponding properties are revealed by the time integral ΔCa_{OS} of the net Ca^{2+} efflux, which is plotted in Fig. 8 *b* as a function of time after the flash. It is obvious that the magnitude of ΔCa_{OS} is dependent on the external Ca^{2+} concentration, whereas the time course is not. It is noteworthy that this experiment shows again only half of the released Ca^{2+} to be taken back up by the outer segment (cf. also Fig. 7 *c*).

In Fig. 8 *c*, the maximum of the net Ca^{2+} efflux Q_{OS}^{max} as well as the maximum of Ca^{2+} extruded from the outer segment, ΔCa_{OS}^{max}, are plotted in dependence of the extracellular Ca^{2+} concentration. In this diagram, the corresponding Q_o values of the initial net Ca^{2+} efflux, which are derived as described in the next section, are also plotted. All three quantities show a nearly linear increase with the Ca^{2+} concentration in Ringer's solution.

Variation of Flash Intensity and Temperature

Fig. 9 represents the net Ca^{2+} efflux Q_{OS} from the outer segment and the respective photosignals determined at 23 and 30°C. Saturating flashes exciting 600 and 3,000 R*/ros were used. The maximum Ca^{2+} efflux Q_{OS}^{max} appears with a distinct delay of 0.5–1.0 s after the saturating flash. On the other hand, Miller and Korenbrot (1987) showed a net Ca^{2+} efflux from amphibian rod outer segments which rises instantly, i.e., within at least 0.1 s after a saturating flash to a maximum value. There is no weighty reason as yet to assume that the net Ca^{2+} efflux in mammalian rods rises much slower. Therefore, the delayed appearance of Q_{OS}^{max} as shown in Fig. 9 should be solely due to the band width limitation caused by the Ca^{2+}-sensitive electrode and the smoothing procedure.

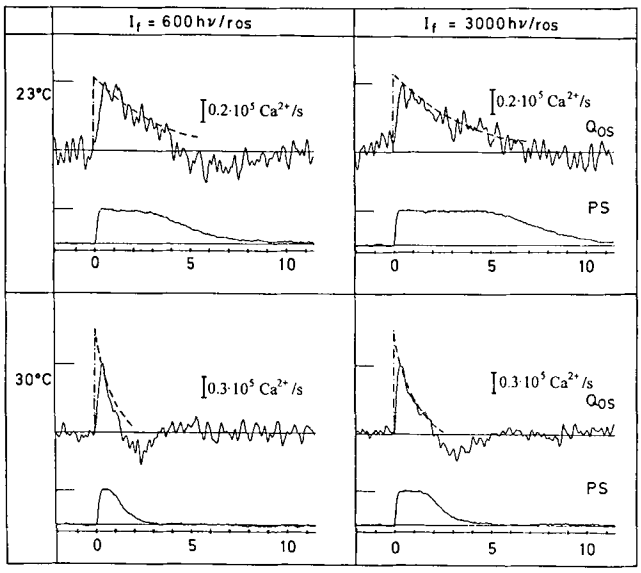

FIGURE 9. Photosignals (*PS*) and the corresponding net Ca^{2+} efflux from the whole outer segment (Q_{OS}) are shown at temperatures of 23 and 30°C in response to flashes exciting 600 and 3,000 R*/ros, respectively. The Ringer's solution contained 250 μM Ca^{2+}. The data were obtained from one and the same piece of retina. An exponential decay curve was fitted to the Ca^{2+} efflux signals Q_{OS} (----). The vertical lines (–·–) represent the instantaneous increases of Q_{OS} that would be obtained if there were no band limitations present (cf. Eq. 11). The fitted values for Q_0 and τ_Q are given in Table II.

Therefore, the actual net Ca^{2+} efflux Q_{OS} was approximated by a maximum initial value Q_o, which is reached instantly after the flash at $t = 0$ and decays exponentially to zero with a time constant τ_Q as long as the Ca^{2+} influx is completely suppressed:

$$Q_{OS} = Q_o e^{-t/\tau_Q} \tag{11}$$

Instead of Eq. 11, according to the bandwidth limitation characterized by an effective time constant τ_B, the measured Q_{OS} signal is more accurately described by

$$Q_{OS} = Q_o \frac{\tau_Q}{\tau_Q - \tau_B}\left(e^{-t/\tau_Q} - e^{-t/\tau_B}\right). \tag{12}$$

In principle, Q_o and τ_Q can be derived from the given Q_{OS} data by fitting Eq. 12 to the first part of the signals shown in Fig. 9 or 7 *b*. However, according to the low S/N ratio of these signals, the data obtained by this curve fitting procedure are subject to considerable error. Thus, for data evaluation, the following approximation procedure was used: As shown in Fig. 9 by dashed lines, monoexponential curves were fitted to the measured Q_{OS} signals in the time period between t_{max} and three to four times t_{max}. The initial value Q_o of the Ca^{2+} efflux was then determined by extrapolating the exponential fit curve to $t = 0$, i.e., to the moment the flash was applied. By model calculation, it was

TABLE II

Characteristic Data of the Net Ca^{2+} Efflux from the Rod Outer Segment

	I_f	Q_{OS}^{max}	Q_0	ΔCa_{OS}^{max}	τ_Q	ΔCa_{OS}^{∞}
	R/ros*	$10^4 \cdot Ca^{2+}/s$	$10^4 \cdot Ca^{2+}/s$	$10^4 \cdot Ca2^+$	*s*	$10^4 \cdot Ca^{2+}$
23°C	3000	5.8	6.9	16.0	3.4	23.4
	600	5.9	7.0	14.0	3.4	23.9
30°C	3000	9.5	14.8	9.6	0.8	11.8
	600	9.2	15.9	6.1	0.8	12.7

Evaluation of the time course of net Ca^{2+} efflux $Q_{OS}(t)$ shown in Fig. 9. Q_{OS} (*t*) was determined in response to flashes that produced 600 and 3,000 *R**/ros at 23 and 30°C, respectively. The maximum value Q_{OS}^{max} of the net Ca^{2+} efflux, the initial value Q_o of the net Ca^{2+} efflux (see text), and time constant τ_Q of its exponential decline are listed as well as ΔCa_{OS}^{max}, which is the maximum amount of Ca^{2+} ions actually extruded per photoresponse and ΔCa_{OS}^{∞}, which is an estimation of the amount of Ca^{2+} ions the $Na^+/K^+ - Ca^{2+}$ exchanger is maximally able to pump out ot the outer segment if the Ca^{2+} efflux is indefinitely suppressed (see text).

TABLE III

Ca^{2+} Fraction of Ions Carrying the Dark Current of the Rat Rods

Ca_o	Q_o	j^d	j_{Ca}/j^d
μM	$10^5 Ca^{2+}/s$	pA	%
100	3.2	9.2	1.15
200	4.2	7.7	1.8
500	5.3	5.0	3.5
1,000	11.7	4.6*	8.5

The fraction of the dark current j_{Ca}/j^d carried by Ca^{2+} ions at 30°C is estimated for one retina at different Ca^{2+} concentrations $[Ca]_o$ in the extracellular Ringer's solution as described in the text. Q_o is the net Ca^{2+} efflux extrapolated to $t = 0$; i.e., the moment the flash is applied, and j^d is the dark current. j_{Ca} was calculated assuming that Q_o equals the effective Ca^{2+} influx in the dark (see text). Then, $j_{Ca} = 2e_0 \cdot Q_o$ with e_0 = electronic charge. *Taken from Robinson et al. 1993. To obtain the other dark current values j^d, saturated photosignals were measured at different levels of $[Ca]_o$. The maximum amplitude of these signals was related to the dark current amplitude given by Robinson.

shown that, by this simple approximation, even in the most unfavorable case $\tau_B = \tau_Q$, the extrapolated value of Q_{OS} is only slightly underestimated (down to maximally −30%), whereas the time constant τ_Q is overestimated (up to maximally 35%).

The results of the signal data evaluation are summarized in Table II: The maximum of the net Ca^{2+} efflux, Q_{OS}^{max}, as well as the time constant τ_Q of its exponential decay, are dependent on the temperature and independent of the flash intensity I_f. From the $Q_{OS}(t)$ traces represented in Fig. 9, the maximum rate Q_{OS}^{max} of the Ca^{2+} efflux from the outer segment was determined to be in the average $\sim 6 \cdot 10^4$ and $9 \cdot 10^4$ Ca^{2+}/s, and the time constant τ_Q was determined to be 3.4 and 0.8 s at a temperature of 23 and 30°C, respectively. The average value of the time constant was 4.2 (±1.2 SD, $n = 5$) s at 23°C and 1.0 (±0.2 SD, $n = 4$) s at 30°C, showing a temperature dependence corresponding to an activation energy of 150±45 kJ/mol. Thus, at the physiological temperature of 37°C, the decay time is calculated to be $\tau_Q = 0.3$ s.

Initial values Q_o are given in Table II for temperatures of 23 and 30°C and in Table III also for different values of the external Ca^{2+} concentration. As expected, it is evident from Table II that, like Q_{OS}^{max}, the initial value Q_o is also independent of the flash intensity but rises with temperature and, according to Fig. 8 *c*, also with the external Ca^{2+} concentration.

The maximum amount of Ca^{2+} ions, ΔCa_{OS}, that the Na^+/K^+–Ca^{2+} exchanger is able to pump out of the outer segment if the Ca^{2+} influx is indefinitely suppressed, i.e., if no Ca^{2+} flows back, is obtained by the infinite time integration of Eq. 11, $\int_0^\infty Q_{OS} dt$ yielding

$$\Delta Ca_{os}^{\infty} = \tau_Q \cdot Q_o. \quad (13)$$

Calculated values of ΔCa_{OS}^{∞} are given in Table II. It is noteworthy that ΔCa_{OS}^{∞} is reduced by ~55% if the temperature is increased from 23 to 30°C.

Determination of Net Ca^{2+} Efflux from the Outer Segment at Steady Light

After the onset of a constant illumination, only a transient increase of the extracellular Ca^{2+} concentration was expected. After some time of saturating illumination, the outer segments were expected to lose their Ca^{2+} contents completely so that the Ca^{2+} efflux should vanish. Thereupon, the elevated concentration between the photoreceptors should disappear because by diffusion, the Ca^{2+} ions should be equally distributed within the Ringer's solution.

Contrary to expectations, a constant rise of the extracellular Ca^{2+} concentration is produced by illuminating the retina with steady light. Such a continuous elevation could reliably be detected at least up to 5 min. An experiment performed with continuous illumination is shown in Fig. 10: The retina was illuminated for 10.5 s with steady light that completely shuts off the dark current (*a*). The external Ca^{2+} concentration (*b*) is permanently elevated by ~2 μM, indicating a continuous net Ca^{2+} efflux from the outer segments during steady illumination. The net Ca^{2+} efflux (*c*) corroborates this indication: The Ca^{2+} efflux from the outer segment rises to a maximum value after the onset of the illumination and subsequently declines exponentially to a resting level, which by exponential curve fitting was found to be ~13% of the maximum value. The values of the maximum Ca^{2+} efflux ($1.5 \cdot 10^5$ Ca^{2+}/s) and the time constant of the exponential decline (τ_Q = 2.3 s) are of the same order of magnitude as those obtained using saturating flashes. The corresponding amount of extruded Ca^{2+}, ΔCa_{OS}, is shown in Fig. 10 *d*. It is striking that, after switching off the light, only 30% of the Ca^{2+} extruded before from the outer segment is restored. That means the Ca^{2+} deficiency of the outer segment is higher after long-lasting steady illumination than after intense saturating flashes (cf. 50% in Fig. 8 *b*).

DISCUSSION

The light-induced reduction of the photovoltage that is proportional to the dark current and the increase of the Ca^{2+} concentration were measured extracellularly in the photoreceptor layer of the albino rat retina. For stimulation, flashes and steady light were used. By applying the one-dimensional diffusion equation (Eq. 4) to the measured data, the Ca^{2+} source function and the corresponding net Ca^{2+} efflux along the rod were directly derived. Unlike the study of Yoshikami et al. (1980), it was not necessary to make simplifying assumptions concerning the distribution of Ca^{2+} sources along the rod and about the extracellular space in the photoreceptor layer .

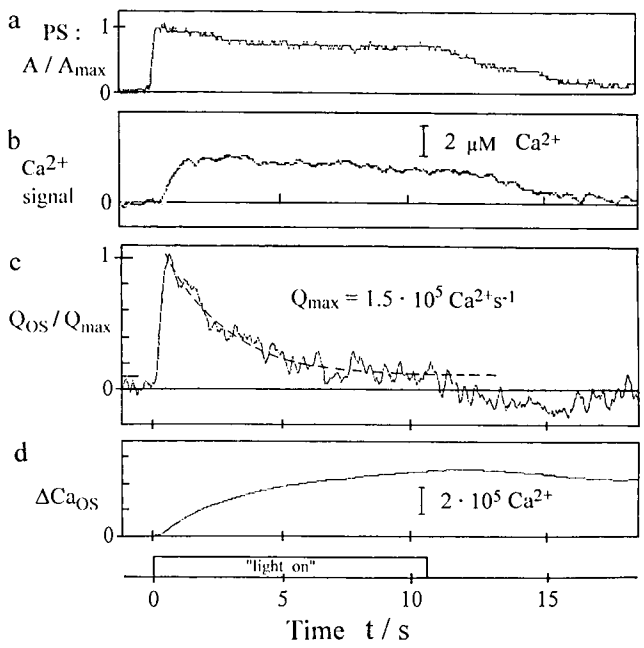

FIGURE 10. (*a*) Photosignal (*PS*), (*b*) Ca^{2+} signal simultaneously measured at a position $z = 30$ μm. (*c*) Net Ca^{2+} efflux Q_{OS} determined for the whole outer segment, and (*d*) ΔCa_{OS}, amount of Ca^{2+} extruded from the outer segment. The retina was illuminated by steady light of saturating intensity over a time period of 10.5 s (indicated by a bar). The Ringer's solution contained 250 μM Ca^{2+}. A curve fitting of trace *c* results in an exponential decline of $Q_{OS}(t)$ with $\tau = 2.3$ s towards a residuum value of $(2\pm1) \cdot 10^4$ Ca^{2+}/s. Temperature, 30°C.

The method used in this study enables the determination of Ca^{2+} fluxes through the plasma membrane at distinct positions of the rods during a complete photoresponse. By this method, at an extracellular Ca^{2+} concentration of 250 μM, fluxes down to $1 \cdot 10^3$ Ca^{2+}/s per μm rod length (cf. Fig. 6) or $2 \cdot 10^4$ Ca^{2+}/s per rod outer segment (cf. Figs. 7 and 9) could be resolved. The latter is equivalent to an exchange current of 3 fA per rod if one allows for a transport of one electronic charge per Ca^{2+} transport. Therefore, even small Ca^{2+} fluxes could be measured which cannot be resolved by suction electrodes having a resolution ≥200 fA (Miller and Korenbrot, 1987; Nakatani and Yau, 1988; Tamura et al., 1991).

Our investigations of rat rods reveal Ca^{2+} fluxes that to a large extent behave similarly to those in amphibian rods. However, there are some discrepancies and certain important new findings.

Light-induced Reduction of the Ca^{2+} Concentration in the Outer Segment

In the dark, there is no net Ca^{2+} efflux from the outer segment. This is indicated for instance by the prestimulus zero value of Q_{OS} shown in Fig. 10 *c*. Moreover, if the Ca^{2+} sensitive electrode is inserted in the dark into the photoreceptor layer, there is no Ca^{2+} gradient to be detected between the outer segment region and the Ringer's solution above the retina (Rüppel and Cieslik, 1988). This is presumed to be due to a balance between a Ca^{2+} influx through the cGMP-dependent membrane channels and a Ca^{2+} efflux via the Na^+/K^+–Ca^{2+} exchanger (Yau and Nakatani, 1985; Miller and Korenbrot, 1987). When exposed to light, however, a net Ca^{2+} efflux is evoked from the outer segment, i.e., the Ca^{2+} efflux exceeds the Ca^{2+} influx. This is indicated by the increase of the extracellular Ca^{2+} concentration and is directly shown by the source function rising from zero to positive values. Most probably, the light-induced net Ca^{2+} efflux is almost exclusively due to a reduced Ca^{2+} influx.

To study the Ca^{2+} fluxes in more detail, flashes of increasing light intensity were applied to the rat retina. In Fig. 5 it is shown that the net Ca^{2+} efflux approaches a maximum value if the maximum amplitude of the photosignal reaches the saturating level. In this case, the Ca^{2+} influx through the membrane channels into the outer segment is completely interrupted. This result agrees with findings of Gold (1986) and Miller and Korenbrot (1987), who also obtained a maximum Ca^{2+} efflux from amphibian rods when all of the Na^+ channels close after a saturating flash.

The maximum of the net Ca^{2+} efflux appears immediately after a saturating flash. Subsequently, as long as the dark current is shut off, the Ca^{2+} efflux decays exponentially (see Figs. 7 and 9). The maximum value and the time constant of the exponential decline are independent of the saturating flash strength. During this period of time, the Ca^{2+} influx is completely interrupted. Thus, the exponential decline of the net Ca^{2+} efflux might be due to a corresponding exponential reduction of the free Ca^{2+} concentration in the outer segment (see also Miller and Korenbrot, 1987), since the magnitude of the Ca^{2+} extrusion is found to be proportional to the free cytoplasmic concentration (Lagnado et al., 1988).

A reduced Ca^{2+} concentration in the outer segments becomes apparent, indeed, when the cGMP-dependent membrane channels reopen. Then the outer segment acts as a sink so that the Ca^{2+} concentration near the outer segment falls even below the dark level. Obviously, the Ca^{2+} influx exceeds the Ca^{2+} efflux at this stage. This is the result of a decreased Ca^{2+} efflux caused by a reduced Ca^{2+} concentration in the outer segment. Other explanations of the transient appearance of sinks may be a light-induced increase of Ca^{2+} permeability of the membrane channels or an inhibition of the Na^+/K^+–Ca^{2+} exchange mechanism. However, at present there is no indication for either. As shown below, the Ca^{2+} permeability stays constant.

By means of the Ca^{2+} influx exceeding the Ca^{2+} efflux, the reduced intracellular Ca^{2+} concentration is restored. When the free Ca^{2+} concentration in the outer segment reaches the dark level, the Ca^{2+} influx and efflux are balanced again.

In summary, the results presented here agree with the notion that light decreases the Ca^{2+} influx through the cGMP-dependent ion channels, whereas the photoresponse, the undiminished Ca^{2+} efflux via the Na^+/K^+–Ca^{2+} exchanger reduces the Ca^{2+} concentration in the outer segment. The results obtained here from rat rods are in accordance with the present concept for the light-induced changes of Ca^{2+} fluxes across the plasma membrane of amphibian rods. Therefore, it seems to be feasable to apply to these data of rat rods a model that was discussed for ion fluxes in amphibians (Miller and Korenbrot, 1987). In this model the Ca^{2+} influx (J_{in}) is assumed to parallel the dark current, whereas the Ca^{2+} efflux (J_{eff}) via the Na^+/K^+–Ca^{2+} exchanger is proportional to the free Ca^{2+} concentration $[Ca]_f$ in the outer segment and is affected by hyperpolarization. As the net Ca^{2+} efflux Q_{OS} is the sum of Ca^{2+} in- and efflux, $Q_{OS} = J_{in} + J_{eff}$, the Ca^{2+} efflux J_{eff} can be readily deduced from Q_{OS} (Fig. 7 *b*) by subtracting the Ca^{2+} influx J_{in}, which corresponds to the photosignal (Fig. 7 *a*, see legend of Fig. 7 *b* for the scaling factor). The Ca^{2+} efflux J_{eff} provides the free Ca^{2+} concentration $[Ca]_f$ after a saturating flash (Fig. 7 *d*), which is exponentially reduced to a minimum of ~35% of the dark value $[Ca]_f^d$. This result fits well with fluorochromic measurements of the free intracellular Ca^{2+} concentration with Fura II of Ratto et al. (1988) but partially disagrees with recent results of McCarthy et al. (1994).

Contribution of Ca^{2+} to the Dark Current

At an external Ca^{2+} concentration of 1 mM, the fraction of the dark current carried by Ca^{2+} is reported to be 10–15% for amphibian (Nakatani and Yau, 1988; Hodgkin et al., 1987) as well as for mammalian rods (Tamura et al., 1991). Decreasing the extracellular Ca^{2+} concentration to 0.1 mM reduces the contribution of Ca^{2+} to the dark current to 1.9%, suggesting a strong dependence on the external Ca^{2+} concentration (Miller and Korenbrot, 1987).

The Ca^{2+} contribution to the dark current can be estimated by determining the dark value of the Ca^{2+} influx into the outer segement. In the dark, the Ca^{2+} influx J_{in} is equal to the Ca^{2+} efflux J_{eff}. Thus, the Ca^{2+} influx in the dark can be obtained by extrapolating the net Ca^{2+} efflux decaying exponentially after the flash back to $t = 0$, i.e., to the time the flash is applied. A result for one retina is shown in Table III. The initial net Ca^{2+} efflux $Q_0 = J_{in}$ is given together with the dark current and its Ca^{2+} fraction. It is obvious that the dark current j^d decreases if the Ca^{2+} concentration in Ringer's solution is increased. This finding was reported already by Hagins (1970). The Ca^{2+} fraction of the dark current, however, is found to rise approximately linearly with the Ca^{2+} concentration in Ringer's solution. A tenfold concentration increase from 0.1 to 1 mM causes this fraction to rise by nearly a factor of ten, too. This result indicates that the ratio of permeabilities for Ca^{2+} and Na^+ ions is unchanged in the light-regulated ion channels, at least under the conditions of these experiments. Obviously, the increase of the dark current after lowering the extracellular Ca^{2+} concentration is exclusively due to a reduced intracellular Ca^{2+} concentration, leading to an increased cGMP concentration probably by a stimulation of the GC. The channel selectivity seems to be unaffected.

These results from rat rods agree with those of Miller and Korenbrot (1987) obtained from the tiger salamander. Furthermore, it is evident from these new data that an external Ca^{2+} concentration of 1 mM is necessary to obtain a Ca^{2+} fraction of the dark current of ~10% for mammalian rods also.

Dependence of Maximum Net Ca^{2+} Efflux on the External Ca^{2+} Concentration

As shown in Table III, the initial maximum Ca^{2+} efflux Q_0 from the outer segment decreases by a factor of 3.6 if the Ca^{2+} concentration in the Ringer's solution is reduced from 1 to 0.1 mM. This should correspond to a decrease of the Ca^{2+} influx in the dark by the same amount. As the Ca^{2+} efflux is proportional to the free Ca^{2+} concentration $[Ca]_f$ in the outer segment (Lagnado et al., 1988), $[Ca]_f$ should be small compared with the K_m value for the Ca^{2+} extrusion by the Na^+/K^+–Ca^{2+} exchanger. Thus, the observed decrease of the maximum Ca^{2+} efflux should indicate that the dark value of the free Ca^{2+} concentration $[Ca]_f^d$ has dropped by a factor of 3.6 as well. This is valid only if the internal concentrations of Na^+ and K^+ as well as the membrane voltage remain unaffected by the alteration of the external Ca^{2+} concentration. Actually, however, decreasing the external Ca^{2+} concentration increases the dark current. As a consequence, the Na^+ concentration in the outer segment should be elevated. This in turn would result in a deactivation of the Na^+/K^+–Ca^{2+} exchange mechanism (Hodgkin and Nunn, 1987) so that the decreased Ca^{2+} efflux could be attributed also to a rise of the Na^+ concentration in the outer segment. On the other hand, an evaluation of the $Q_{OS}(t)$ traces as shown in Fig. 8 *a* yielded the rate constant $1/\tau_Q$ of the Ca^{2+} extrusion to be independent of the external Ca^{2+} concentration. Because $1/\tau_Q$ depends on the internal Na^+ concentration (Hodgkin and Nunn, 1987), this finding suggests that the internal Na^+ concentration remains unaffected by an increase of the external Ca^{2+}

concentration $[Ca]_o$. Thus, as a conclusion, the decrease of the Ca^{2+} efflux can be regarded to be mainly due to a fall of the free intracellular Ca^{2+} concentration $[Ca]_i^d$.

Recent measurements in amphibian rod outer segments revealed $[Ca]_i^d$ to be ~300–400 nM at an external Ca^{2+} concentration of 1 mM (Miller and Korenbrot, 1989; Lagnado et al., 1992). It must be emphasized that this result is quite difficult to obtain. For the much smaller mammalian rods, the corresponding data are not yet available. Now, as several properties of amphibian and mammalian rods are shown to agree (Nakatani et al., 1991; Tamura et al. 1991), it may be justified to assume that $[Ca]_i^d$ in rat rods is not much different from that in amphibian rods. Therefore, if reduced by a factor of 3.6 when lowering the extracellular Ca^{2+} concentration from 1.0 to 0.1 mM, $[Ca]_i^d$ should drop in the rat rod outer segment from 300–400 nM to 80–110 nM. The lower value seems to be relatively unlikely because, according to Koch and Stryer (1988), the GC should be close to full activation at $[Ca]_i^d = 80$ nM. However, such a GC activation should increase the cGMP level dramatically, followed by an opening of additional membrane channels and a considerable inflow of Na^+. The resulting increase of the dark current should by far overcome the observed value (cf. Table III). Furthermore, no efficient desensitization would be expected in the rod receptor at $[Ca]_o < 0.1$ mM. Actually, however, an effective adaptation is still observed at this external Ca^{2+} concentration. In summary, it seems to be more realistic to assume the upper limit of 400 nM to be the dark value of $[Ca]_i$ at $[Ca]_o = 1$ mM. In this case, $[Ca]_i^d$ is reduced only to 110 nM so that nothing but a moderate GC activation is expected if the external Ca^{2+} concentration is reduced from 1 to 0.1 mM.

Dependence of the Net Ca^{2+} Efflux on the Temperature

According to Table II, the maximum of the net Ca^{2+} efflux as well as its exponential decline in time are strongly temperature dependent. If the temperature is raised from 23 to 30°C, the maximal Ca^{2+} efflux increases on the average by 70%, whereas the decay time constant is reduced by ~25%. It is well known that a rise in temperature increases the dark current (Penn and Hagins, 1972; Robinson et al., 1993). If the Ca^{2+} selectivity of the ion channels remains unaffected, an increased dark current implies an enhanced Ca^{2+} influx into the outer segment. However, this need not lead to an increased dark level of the free Ca^{2+} concentration $[Ca]_i^d$ if the increase in the dark current is accompanied by a temperature-dependent activation of the Na^+/K^+–Ca^{2+} exchange mechanism. Moreover, if the activation of the Ca^{2+} efflux exceeds the enhancement of the Ca^{2+} influx, the dark level $[Ca]_i^d$ would even fall. In any case, an increased peak maximum of the net Ca^{2+} efflux would be expected.

As the exponential decline of the net Ca^{2+} efflux occurs only during completely interrupted dark current its time constant is solely dependent on the activity of the Na^+/K^+–Ca^{2+} exchanger. Thus, the large temperature change of the decay rate $1/\tau_Q$, which corresponds to an activation energy of 150 kJ/mol, must be due to the temperature dependence of the exchanger activity. The much smaller temperature dependence of the maximal Ca^{2+} efflux Q_o, however, is due to the fact that Q_o represents the dark equilibrium between Ca^{2+} in- and efflux and thus reflects the combined temperature dependencies of both processes.

Deficiency in the Balance of Ca^{2+} Fluxes

By numerous experiments, it has been repeatedly shown (cf. Figs. 6–8) that only a fraction of the Ca^{2+} released during a photoresponse will be taken back up by the rod outer segment when the dark-adapted state is reached again. This unexpected effect is observed if light stimulation is achieved either by a saturating flash (Fig. 9) or by a saturating long pulse of steady light (Fig. 10). Apparently, saturating light stimulation induces an irreversible loss of Ca^{2+} ions from the outer segment.

Such an irreversible light-induced loss of Ca^{2+} from the outer segment of the rat rod has only been reported before by Yoshikami et al. (1980), who used similar experimental conditions. However, such an effect was not obtained from rods or retinae of amphibians (Miller and Korenbrot, 1987; Gold, 1986). This discrepancy may be due to the different methods used or to differences between species.

Actually, the Ca^{2+} deficiency in the rod outer segment detected by applying strong flashes amounts to ~50% (cf. Figs. 7 and 8). A higher deficiency, however, was evoked by long-lasting and saturating steady light (e.g., 70% in Fig. 10 *d*). The largest deficiency measured in this study was as high as 95%. Therefore, the magnitude of the deficiency is obviously dependent on the duration of the plateau phase of the saturating photoresponse and is thus related to the amount of Ca^{2+} extruded during this time period (cf. Fig. 10).

During long periods of continuously interrupted dark current, another phenomenon that is probably correlated with the irreversible Ca^{2+} release becomes evident: After very intense flashes (see Fig. 5 *b*) and during saturating steady light (see Fig. 10 *b*), a constantly elevated Ca^{2+} concentration is observed in the extracellular space between the rod outer segments, indicating a continuous Ca^{2+} release from the outer segment. Correspondingly, the net Ca^{2+} efflux during steady light does not disappear but resumes a residual value (see Fig. 10 *c*, extrapolation).

The origin of these two conspicuous findings is yet to be established. On the basis of the various results obtained in this study, we suggest, that during a photo response, Ca^{2+} is liberated from large internal stores within the rod into the cytoplasma of the outer segment. From there, the Ca^{2+} ions are extruded into the extracellular space. A part of these stores is assumed to release Ca^{2+} irreversibly by this process. The residual Ca^{2+} efflux during steady light as shown in Fig. 10 *c* is suggested to reflect the irreversible Ca^{2+} extrusion.

An estimation may confirm this suggestion and give indications to distinguish between reversible and irreversible Ca^{2+} extrusion during long term steady illumination. In Fig. 10 *d*, ~70% or $3.5 \cdot 10^5$ of the Ca^{2+} ions extruded from the outer segment appear to be irreversibly released. Supposing that Ca^{2+} is irreversibly extruded at a constant rate during the whole time period of the dark current reduction (~13 s), the mean rate of irreversible Ca^{2+} release amounts to $3.5 \cdot 10^5/13$ s = $2.7 \cdot 10^4$ Ca^{2+}/s. In fact, this value corresponds quite well with the residual Ca^{2+} extrusion rate of $(2\pm1)\cdot10^4$ Ca^{2+}/s, which is derived from Fig. 10 *c*. Thus, it is concluded that the residual Ca^{2+} efflux might be due to the irreversible Ca^{2+} release, whereas the exponentially decaying peak initially superposed to the residual efflux should represent the reversible Ca^{2+} extrusion.

In more detail, the following mechanisms may account for an irreversible Ca^{2+} liberation into the cytoplasma during a photoresponse: (*a*) Endogenous Ca^{2+} buffers within the outer segment release Ca^{2+} either irreversibly or, after the release, the buffers rebind Ca^{2+} very slowly. (*b*) The disks in the outer segment act as Ca^{2+} stores and release Ca^{2+} irreversibly or they take up Ca^{2+} very slowly. Actually, these disks are known to contain large amounts of Ca^{2+} (Hagins and Yoshikami, 1975; Somlyo and Walz, 1985; Fain and Schröder, 1985). (*c*) The inner segment acts as a Ca^{2+} store: Ca^{2+} ions diffuse from the inner to the outer segment driven by a Ca^{2+} gradient caused by the light-induced reduction of the free Ca^{2+} concentration in the outer segment. The Ca^{2+} gradient is maintained by a slightly higher Ca^{2+} concentration in the inner segment, kept constant by a Ca^{2+} release from the mitochondria or the endoplasmatic reticulum. Both cell bodies are known to contain large amounts of Ca^{2+} ions (Somlyo and Walz, 1985; Ungar et al., 1984). (*d*) An influx of Ca^{2+} ions from the extracellular space into the inner segment is followed by a diffusion into the outer segment, from which they are extruded again into the interstitial space. Thus, during a photoresponse, a circulating flow of Ca^{2+} ions results between the outer and inner segment that is opposite to the circulating Na^+ current in the dark.

At present, it is not possible to favor one of these mechanisms (*a–d*) because little is known about the distribution and the light-induced fluxes of Ca^{2+} ions within the rod. Nevertheless, several results support a diffusion of Ca^{2+} ions from the inner to the outer segment during a photoresponse. The major deficiency of Ca^{2+} was measured in the middle and at the proximal end of the outer segment, whereas there is almost no deficiency at the tip of the outer segment, most distant from the inner segment (see Fig. 6 *b*). This means that most of the irreversibly released, i.e., not reentered, Ca^{2+} ions were extruded from the part of the outer segment that is next to the inner segment. This should be expected if the inner segment is the source of the irreversible Ca^{2+} liberation as suggested by mechanism *c*.

Furthermore, as shown in Fig. 6 *a* during the first 3–4 s after the flash, Ca^{2+} sinks are revealed along the inner segment whereas Ca^{2+} sources are observed along the outer segment. This is in accordance with mechanism *d*.

On the other hand, the Ca^{2+} extrusion experiments with steady light (Fig. 10) do not disprove unequivocally the possibility that the Ca^{2+} buffers in the outer segment might be the source for the observed Ca^{2+} deficiency as postulated in models *a* and *b*. This is easily shown by the following estimation: Adopting a buffer capacity of 2 Ca^{2+}/rhodopsin (Hagins and Yoshikami, 1975; Schröder and Fain, 1985; Rüppel and Hedrich, unpublished results, 1988), one obtains for the rat rod ~10^8 Ca^{2+}/rod. Most probably, the disks contain the great majority of Ca^{2+} in the outer segment. This Ca^{2+} reservoir is by far large enough to account for the observed Ca^{2+} deficiency but also for the residual Ca^{2+} efflux detected over a time period of 5 min at most. At the residual efflux rate of $2 \cdot 10^4$ Ca^{2+}/s as given in Fig. 10 *c*, this reservoir cannot be depleted within a time span of ~1 h.

Furthermore, assuming that during continuous illumination the residual Ca^{2+} efflux of $(2\pm1) \cdot 10^4$ Ca^{2+}/s is caused by a Ca^{2+} release from the disks, for 750 disk per rat rod, one obtains an extrusion rate per disk of 15–45 Ca^{2+}/s. This value is of the same order of magnitude as the rate of Ca^{2+} exchange in the disks of ~100 Ca^{2+}/s per disk, which was found by Fain and Schröder (1987) for the toad retina of *Bufo marinus* in the dark.

Finally, a constant increase of the extracellular Ca^{2+} concentration during steady light as shown in Fig. 10 *b* has also been observed by Livsey et al. (1990) in the isolated frog retina. However, if the pigment epithelium was not removed from the photoreceptor layer, an initial increase of the extracellular Ca^{2+} concentration after the onset of steady light was followed by a slow reduction even below the dark level. Therefore, a light-induced Ca^{2+} influx into the pigment epithelium was assumed (Livsey et al., 1990). Obviously, in vivo, during constant illumination the permanent Ca^{2+} efflux from the outer segment feeds a Ca^{2+} current from the outer segment into the pigment epithelium. Because it is a

well-known fact that all *trans* retinal has to be transferred to the pigment epithelium for regeneration (Rando, 1990; Saari, 1990), it may be speculated that the retinal transport is governed by this light-induced Ca^{2+} current.

The authors thank Professor I. Pommerening (Free University of Berlin, Berlin, Germany) for his assistance during textual revision.

This work was supported by the Deutsche Forschungsgemeinschaft (Bonn, Germany) projects Ru 209, 9-6 and 13-1.

Original version received 23 February 1995 and accepted version received 12 February 1996.

REFERENCES

Allen, M.P., and D.J. Tildesley. 1987. Computer simulation of liquids. Oxford University Press, New York.

Cervetto, L., L. Lagnado, R.J. Perry, D.W. Robinson, and P.A. McNaughton. 1989. Extrusion of calcium from rod outer segments is driven by both sodium and potassium gradients. *Nature (Lond.).* 317:740–743.

Fain, G.L., and W.H. Schroeder. 1985. Calcium content and calcium exchange in dark adapted toad rods. *J. Physiol. (Camb.).* 368: 641–655.

Fain, G.L., and W.H. Schroeder. 1987. Calcium in dark-adapted toad rods: evidence for pooling and guanosine-3′-5′-monophosphate-dependent release. *J. Physiol. (Camb.).* 389:361–384.

Friedel, U., G. Wolbrink, P. Wohlfahrt, and N.J. Cook. 1991. The Na^+/Ca^{2+}-exchanger of bovine rod photoreceptors: K^+-dependence of the purified and reconstituted protein. *Biochim. Biophys. Acta.* 1061:247–252.

Gold, G.H. 1986. Plasma membrane calcium fluxes in intact rods are inconsistent with the "calcium hypothesis." *Proc. Natl. Acad. Sci. USA.* 83:1150–1154.

Hagins, W.A. 1970. The visual process: excitatory mechanisms in the primary receptor cells. *In* Annual Review of Biophysics and Bioengineering. 1:131–158.

Hagins, W.A., R.D. Penn, and S. Yoshikami. 1970. Dark current and photo current in retinal rods. *Biophys. J.* 10:380–412.

Hagins, W.A., and S. Yoshikami. 1975. Ionic mechanisms in excitation of photoreceptors. *Ann. NY Acad. Sci.* 264:314–325.

Hodgkin, A.L., P.A. McNaughton, and B.J. Nunn. 1985. The ionic selectivity and calcium dependence of the light sensitive pathway in rods. *J. Physiol. (Camb.).* 358:447–468.

Hodgkin, A.L., P.A. McNaughton, and B.J. Nunn. 1987. Measurement of sodium calcium exchange in salamander rods. *J. Physiol. (Camb.).* 391:347–370.

Hodgkin, A.L., and B.J. Nunn. 1987. The effect of ions on sodium calcium exchange in salamander rods. *J. Physiol. (Camb.).* 391: 371–398.

Hsu, Y.-T., and R.S. Molday. 1993. Modulation of the cGMP-gated channel of rod photoreceptor cells by calmodulin. *Nature (Lond.).* 361:76–79.

Kawamura, S. 1993. Rhodopsin phosphorylation as a mechanism of cyclic GMP phosphodiesterase regulation by s-modulin. *Nature (Lond.).* 362:855–857.

Knopp, A. 1994. Kalziumflüsse, Kanalregulierung und Rhodopsindesaktivierung im Vertebraten-Sehstäbchen. Berichte aus der Biologie. Verlag Shaker, Aachen, Germany. 110 pp.

Knopp, A., and H. Rüppel. 1993. Is the falling phase of the vertebrate photoreceptor response governed by a Ca^{++} dependent decay of the activated state of rhodopsin? *In* Proceedings of the 21st Göttingen Neurobiology Conference. N. Elsner and M. Heisenberg, editors. Georg Thieme, Stuttgart and New York. p. 416.

Koch, K.-W., and L. Stryer. 1988. High cooperative feedback control of retinal rod GC by calcium ions. *Nature (Lond.).* 334:64–66.

Kuhls, R., H. Rüppel, A. Knopp, R. Hagemann, F.-D. Selke, and H.-P. Berlien. 1995. A comprehensive electrophysiological study of vertebrate retinae irradiated by low power IR-laser light did not reveal biostimulative effects. *Biomed. Lett.* 52:7–36.

Lagnado, L., and D.A. Baylor. 1994. Calcium controls light-triggered formation of catalytically active rhodopsin. *Nature (Lond.).* 367:273–277.

Lagnado, L., L. Cervetto, and P.A. McNaughton. 1988. Ion transport by the Na–Ca exchange in isolated rod outer segments. *Proc. Natl. Acad. Sci. USA.* 85:4548–4552.

Lagnado, L., L. Cervetto, and P.A. McNaughton. 1992. Calcium homeostasis in the outer segment of retinal rods of the tiger salamander. *J. Physiol. (Camb.).* 445:111–142.

Lamb, T.D., P.A. McNaughton, and K.-W. Yau. 1981. Spatial spread of activation and background desensitation in toad outer segments. *J. Physiol. (Camb.).* 319:463–496.

Livsey, C.T., B. Huang, J. Xu, and C.J. Karwoski. 1990. Light evoked changes in extracellular Ca^{2+}-concentration in frog retina. *Vision Res.* 30:853–861.

Matthews, H.R. 1991. Incorporation of chelator into guinea-pig rods shows that calcium mediates mammalian light adaptation. *J. Physiol. (Camb.).* 436:93–105.

Matthews, H.R., R.S. Murphy, G.L. Fain, and T.D. Lamb. 1988. Photoreceptor light adaptation is mediated by cytoplasmic calcium. *Nature (Lond.).* 334:67–69.

McCarthy, S.T., J.P. Younger, and W.G. Owen. 1994. Free calcium concentrations in bullfrog rods determined in the presence of multiple forms of Fura II. *Biophys. J.* 67:2076–2089.

Miller, D.L., and J.I. Korenbrot. 1987. Kinetics of light-dependent Ca^{2+} fluxes across the plasma membrane of rod outer segments. *J. Gen. Physiol.* 90:397-425.

Miller, D.L., and J.I. Korenbrot. 1989. Cytoplasmic free calcium concentration in retinal rod outer segments. *Vision Res.* 29:939–948.

Nakatani, K., T. Tamura, and K.-W. Yau. 1991. Light adaptation in retinal rods of the rabbit and two other non-primate mammals. *J. Gen. Physiol.* 97:413–436.

Nakatani, K., and K.-W. Yau. 1988. Calcium and magnesium fluxes across the plasma membrane of the toad rod outer segment. *J. Physiol. (Camb.).* 395:695–729.

Penn, R.D., and W.A. Hagins. 1969. Signal transmission along retinal rods and the origin of the electroretinographic α-wave. *Nature (Lond.).* 223:201–205.

Penn, R.D., and W.A. Hagins. 1972. Kinetics of the photocurrent in

retinal rods. *Biophys. J.* 12:1073–1094.

Pepperberg, D.R., J. Jin, and G.J. Jones. 1994. Modulation of transduction gain in light adaptation of retinal rods. *Visual Neurosci.* 11:53–62.

Pugh, E.N., Jr., and J. Altmann. 1988. A role for calcium in adaptation. *Nature (Lond.).* 334:16–17.

Pugh, E.N., Jr., and T.D. Lamb. 1990. Cyclic GMP and calcium: the internal messengers of excitation and adaptation in vertebrate rods. *Vision Res.* 30:1923–1948.

Rando, R.R. 1990. The chemistry of vitamin A and vision. *Angew. Chem. Int. Ed. Engl.* 29:461–480.

Ratto, G., R. Payne, W.G. Owen, and R.Y. Tsien. 1988. The concentration of cytosolic free calcium in vertebrate ros measured with FURA-2. *J. Neurosci.* 8:3240–3246.

Requena, J. 1983. Calcium transport and regulation in nerve fibers. *Annu. Rev. Biophys. Bioeng.* 12:237–257.

Robinson, D.W., G. Ratto, L. Lagnado, and P.A. McNaughton. 1993. Temperature dependence of the light response in rat rods. *J. Physiol. (Camb.).* 462:465–481.

Rüppel, H., 1983. Methods for measuring fast reactions. *In* Biophysics. W. Hoppe, W. Lohmann, H. Markl, and H. Ziegler, editors. Springer-Verlag Berlin, Heidelberg, New York, Tokyo. 176.

Rüppel, H., and J. Cieslik. 1988. Light stimulated ion fluxes across the plasma membrane of photoreceptors. *Ber. Bunsen-ges. Phys. Chem.* 92:1020–1025.

Rüppel, H., P. Hochstrate, and H.-E. Buchwald. 1978. Eine gepulste Lumineszenzeldiode zur Anregung photochemischer Reaktionen in biologischen Objekten. *Feinwerktechnik und Meßtechnik.* 86:270–272.

Saari, J.C. 1990. Enzymes and proteins of the mammalian visual cycle. *In* Progress in Retinal Research. N. Osborne and J. Chader, editors. Pergamon Press, Oxford. 363–381.

Somlyo, A.P., and B. Walz. 1985. Elemental distribution in *Rana pipiens* retinal rods: quantitative electron probe analysis. *J. Physiol. (Camb.).* 358:183–195.

Tamura, T., K. Nakatani, and K.-W. Yau. 1991. Calcium feedback and sensitivity regulation in primate rods. *J. Gen. Physiol.* 98:95–130.

Ungar, F., I. Picopo, J. Letizia, and E. Holtzman. 1984. Uptake of calcium by the endoplasmic reticulum of the frog photoreceptor. *J. Cell Biol.* 98:1645–1655.

Wagner, U., N. Ryba, and R. Uhl. 1989. Calcium regulates the rate of disactivation and the primary amplification step in visual transduction. *FEBS Lett.* 242:249–254.

Yau, K.-W., and K. Nakatani. 1985. Light induced reduction of cytoplasmic free calcium in retinal rod outer segment. *Nature (Lond.).* 313:579–585.

Yau, K.-W., and K. Nakatani. 1988. Calcium and light adaptation in retinal rods and cones. *Nature. (Lond.).* 334:69–71.

Yoshikami, S., J.S. George, and W.A. Hagins. 1980. Light-induced calcium fluxes from outer segment layer of vertebrate retinas. *Nature (Lond.).* 286:395–398.